IEEE Access
Multidisciplinary | Rapid Review | Open Access Journal

Received April 29, 2022, accepted May 12, 2022, date of publication May 17, 2022, date of current version May 24, 2022.

Digital Object Identifier 10.1109/ACCESS.2022.3175883

A Transmitter Design for the Multi-beam CC-OFDM Azimuth Scanning MIMO Radar

DEVY KUSWIDIASTUTI[1], (Student Member, IEEE), L. P. LIGTHART[2], (Life Fellow, IEEE), AND GAMANTYO HENDRANTORO[1], (Senior Member, IEEE)

[1]Department of Electrical Engineering, Institut Teknologi Sepuluh Nopember, Surabaya 60111, Indonesia
[2]IRCTR, Delft University of Technology, 2628 CD Delft, The Netherlands *(Retired)*

Corresponding author: Gamantyo Hendrantoro (gamantyo@ee.its.ac.id).

This work was supported in part by the Indonesian Ministry of Research, Technology and Higher Education through the 2014–2018 Beasiswa Pendidikan Pascasarjana Dalam Negeri (BPPDN) Scholarship, in part by the 2015 Insentif Riset Sistem Inovasi Nasional (INSINAS) Research Grant, and in part by the 2019 Penelitian Disertasi Doktor (PDD) Research Grant.

ABSTRACT A conventional phased array radar provides a high gain by transmitting coherent signals over a large number of antenna elements. However, it does not provide a full time-on-target because it produces a beam that scans the whole angular view of the radar. This paper describes an implementation of circulating codes (CC) in azimuth scanning MIMO radar that adopts OFDM waveform. The CC MIMO technique can produce a beam toward a certain angle by applying an appropriate delay difference between the MIMO antennas that transmit the same waveform across the azimuth. The adoption of OFDM waveform in the CC MIMO radar, gives the possibility to apply the phase difference for beamforming in the frequency domain of the OFDM signals. CC-OFDM MIMO with spectrum division into sub-bands and use of orthogonal codes, allow for simultaneous transmission of orthogonal OFDM symbols that generate orthogonal beams toward different angles. This strategy makes it possible for the radar system to have multiple and simultaneous beamforming to provide a full-time coverage. Furthermore, the transmission of a series of orthogonal OFDM symbols in each beam enables the detection of long-range targets. By taking as an example the design of long-range surveillance radar, the paper discusses further issues pertinent to the implementation of the CC OFDM MIMO radar, including the beam squinting problem and its remedy, arrangement of the multiple beams, the radar system structure, use of Golay codes for orthogonalization and PAPR mitigation, use of software-defined radar that eliminates the need of amplitude and phase control in each transmitter, transmit scheduling for multi-beam long-range target detection, and multidimensional ambiguity function analysis. The latter indicates that the CC OFDM MIMO radar can achieve a high resolution in angle, range, and velocity, with beam isolation of −30 dB for neighboring beams and co-channel beams.

INDEX TERMS Array signal processing, circulating-codes, Golay-codes, MIMO-radar, multi-beam, OFDM, software-defined-radar, sub-band, space-time codes, surveillance.

I. INTRODUCTION

Most applications of modern radar systems require scanning capability. Scanning radars that employ a mechanical rotator allow for slow scanning with some potential angular inaccuracies due to mechanical errors [1]. Electronic beam scanning can be achieved by phased arrays, removing the need of a mechanical rotator, thereby eliminating the mechanical errors and at the same time reducing the cost. Typical phased array radar transmits coherent signals with high gain antennas with a pencil beam pattern. Phased arrays acquire high directivity and narrow beam by employing a large number of elements, while the scanning capability is obtained by adjusting phase shift difference between elements by means of phase shifters, individually attached to each element [2]. Nevertheless, phased arrays are still undermined by issues arising from the requirement of many phase shifters when a large array is needed to realize high gain, which makes the production cost higher. In addition, when operating in beam-scanning mode, the time-on-target achieved by electronically scanning radars is limited.

Multi-beam radars, in which multiple beams are formed simultaneously and continuously at both the transmitter and the receiver at different angular directions, can eliminate

The associate editor coordinating the review of this manuscript and approving it for publication was Chengpeng Hao.

the aforesaid problem of limited time-on-target. Multi-beam radar technology is beneficial to various radar applications, such as surveillance [3], [4], automotive radar [5], [6], radar imaging [7], [8], joint multiuser communication and radar [9], [10], etc. In this paper, we are interested in multi-beam radar systems capable of covering a large angular swath with contiguous orthogonal beams, each sufficiently narrow to realize a desired angular resolution, capable of detecting the direction, range and Doppler frequency of multiple targets. Multiple simultaneous beams can be generated by employing a number of transceivers operating individually, each attached to an antenna with a beam pointing at a specified direction, in total covering a specified angular range. Such a method offers a limited solution in angular resolution and cost [11]–[13]. When phased arrays are considered, multiple beams can be achieved for instance by involving a Butler matrix [14]–[16], in which the number of beams remains limited. Another alternative is by forming non-overlapping subarrays within the array [17], naturally limiting the achievable beamwidth of each beam and making inefficient use of the available aperture. A third option can be taken by arranging the array into partially or fully overlapping subarrays coupled with the use of orthogonal waveforms, each associated to a generated beam, a solution belonging to the class of the multi-input multi-output (MIMO) radars discussed below.

MIMO radars have developed into a strong contender for multi-antenna radar systems, applying the concept of virtual sensors with orthogonal waveform diversity [18]–[20]. Our interest in MIMO radars in relevance to the problem at hand arises due to their capability to produce multiple orthogonal beams by selecting an appropriate set of waveforms. Several attempts that have been reported involves the use of linear frequency modulated (LFM) waveforms [21]–[23] and frequency diverse array (FDA) [24], [25]. In the former, quasi-orthogonal waveforms is realized by producing LFM waveforms with different bandwidths and frequency offsets following certain criteria. Advantages of this scheme follow from those of LFM radars, but the range-Doppler coupling remains a problem. In the latter, the FDA radars apply a small frequency increment on consecutive elements across the transmit array, which induces range-time-dependent phase shifts to the elements and in turn produces multiple beams. The range-time-dependent beams cause difficulties in detecting a weak target due to the limited time-on-target and, as per the aforementioned objective of this paper, can make the design and implementation of the multi-beam radar more complicated.

Another contending approach to orthogonal waveforms design was proposed by taking on orthogonal frequency division multiplexing (OFDM) waveforms, with the initial purpose being to have an integrated radar and communication systems [26]–[28]. Radar which operate in power efficient mode by using repeated symbols of OFDM MIMO radar has been proposed in [29]. Continuous and simultaneous wideband transmission from multiple antennas can be done by subcarrier interleaving technique [30], and by using a coded OFDM MIMO waveform [31]. A set of orthogonal waveforms can be simply acquired by arranging the allocation of orthogonal subcarriers into different antennas of the MIMO radar system. In this radar, the pulse width or the OFDM symbol duration is obtained as the inverse of the subcarrier spacing.

Another key element of our proposed radar system is the circulating codes (CC), which are applied by imposing a specified delay between successive antennas of a MIMO radar, intended to produce correlated waveforms with the purpose of acquiring better control over the beampattern. CC have been proposed for application in MIMO radars, originally for optimizing low sidelobes in MIMO radars employing LFM waveforms [32], but only recently the CC has gained attention in terms of in-depth analysis of LFM waveform optimization [33]. Later in this paper, it can be seen that CC find a different role as a consequence of their combination with OFDM waveforms.

In this paper, a novel concept of CC-OFDM MIMO[†] radar is proposed as a solution for the wide-scanning multi-beam radar, which is based on the following principles. Firstly, a train of OFDM pulses are transmitted on an array of transmit antennas by means of the CC concept, i.e., by applying some delay difference between successive elements. The use of subcarrier frequencies with uniform frequency spacings in the OFDM pulses translate the inter-element uniform delay differences thanks to CC into multiple overlapping beams pointing at increasing scan angles. In a previous patent [34], simultaneous multiple beams are generated using OFDM multiple antennas being fed at different points along a transmission line providing delay or phase differences between successive antennas, but the use of such a physical delay source limits its capability and flexibility. On the other hand, OFDM signals with various delays can be produced with CC by flexibly exploiting a programmable waveform generator (WG).

In the CC-OFDM MIMO radar, a novel technique can be used further to mitigate beam broadening for large scanning angles. In a way, the strategy of CC-OFDM MIMO radar can be viewed as a realization of hybrid between phased array and MIMO techniques [35], [36]. Herein, the phased array determines the beamwidth and the beam pattern of the whole array, whereas the MIMO radar concept allows multiple beams generation by means of orthogonal waveforms, which in this case results from OFDM signals occupying different sub bands and taking on different codes.

In realizing the beams, phase shifters are not necessary. Instead, feeding can be done by software-defined radio (SDR) hardware attached to each transmit antenna. In various digital

[†]Patents pending for various technologies involved in both transmitter and receiver of this radar, e.g. the system architecture, combined use of array antenna and OFDM with phase correction per sub-carrier to generate multi-beam, combined use of multiple sub-bands and Golay codes to orthogonalize beams and symbols, symbols and frame transmission and reception scheduling, including the low/high-power modes, beam processing at the receiver by parallel processing, range and Doppler processing involving OFDM symbols and frames.

beamforming applications, SDR technology is preferred for its flexibility and low cost [37], [38]. In our case, the SDR implements all baseband processing at the transmitter and the receiver, including generating inter-element delay required for the application of CC at the transmitter. Beamforming design that meets the required maximum beamwidth in the azimuth is achieved by determining the suitable number of elements employed on the horizontal axis. A good beam pattern can be obtained further by employing amplitude tapering distribution across the multi-antenna system, such as the Taylor distribution [2]. To cover a wide angular scanning range with overlapping narrow beams, a large number of beams are required, which in turn require a sufficiently large number of subcarriers, or in other words, a large bandwidth. In order to use efficiently the limited spectrum allocated to the radar operator, sub-band reuse is applied. Each sub-band is shared by multiple non-adjacent beams by adopting orthogonal codes, Golay codes in our case, to achieve orthogonality among beams. Both the sub-band reuse and its shared use by multiple beams with the help of Golay codes, which also helps to minimize the peak-to-average power ratio (PAPR) of the OFDM waveform, are a novel strategy.

Another new strategy is also proposed herein for the detection of range and velocity of a target. Range detection with good signal-to-noise power ratio (SNR) in a beam pointing toward the direction of a target can be achieved by transmitting a frame consisting of a number of OFDM symbols, whose echoes that arrive in overlap at the receiver are orthogonal to each other. This is achieved by extending the use of the Golay codes to orthogonalization of different symbols in a frame in the same beam. Doppler detection can further be accomplished by transmitting a frame of symbols repeatedly for several times, thus allowing the receiver to detect the changes in phase along different frames. The realization of such multi-beam radars that adopts the CC-OFDM MIMO concept also allows for application of further signal processing, such as monopulse processing to determine the angular direction of the target more accurately, but this is beyond the scope of our paper. The CC-OFDM MIMO concept presents a breakthrough in the realization of multi-beam radar in a way that has not been tried before, combining different strategies in a novel way to obtain a powerful wide-scanning multi-beam radar system with simultaneous range and Doppler detection. To describe the whole concept, it is therefore necessary to divide the discussion into two parts. The first part is on the transmitter, which is presented in this paper, whereas the second part deals with the receiver, which is the topic of another paper currently being prepared. In order to clearly and fully describe the concept of CC-OFDM MIMO radar, while at the same time providing a realistic example of its use in a radar application, in the sequel we focus the discussion on the design of a surveillance radar system. In the example, parameters of the CC-OFDM MIMO radars are determined so as to achieve a specified list of mission requirements.

We start the discussion with the motivation and principle of the CC-OFDM MIMO radar in Section II. To better explain the concept, system and processes pertinent with the CC-OFDM MIMO radar, an example of long-range surveillance radar design is introduced in Section III. It is followed by Sections IV-VI that discuss the multi-beam pattern, the PAPR issue and the ambiguity functions, taking the long-range radar case as a reference. Discussions on the design results and the adoption of SDR concept for such radars are given in Section VII, which is followed by conclusions in Section VIII.

II. CC-OFDM MIMO RADAR SYSTEM CONCEPT

A. MOTIVATION

In the following, the potentials of a new type of radar are used for the motivation of this paper. As a start, it is assumed that azimuth beamsteering is implemented using a horizontal linear array. The coherent signal is circulated from one antenna element to another with a relatively small time-delay difference (Δt), made possible by circulating codes (CC) [32], [33], [39]. Hence the transmit signal from the p-th element for a transmit antenna array with an odd number of elements, N_t, can be written as:

$$x_p(t) = x(t - p\Delta t), \quad p = -\frac{N_t - 1}{2}, \ldots, \frac{N_t - 1}{2} \tag{1}$$

The time delay difference of the circulating signal corresponds to a phase difference between the antenna elements at a given frequency:

$$\Delta\varphi = 2\pi f \Delta t \tag{2}$$

It means that the phase steering that is usually provided by a phase shifter at each antenna element now can be realized directly in the waveform produced by a WG and transmitted from the antennas. Consequently, it eliminates the requirement of phase shifter per element and lowers the production cost.

This brings us to the idea of a MIMO structure, where each transmit element is fed by a transmitter with a digital WG which individually responsible for the delay specified for each of them. In addition, the MIMO structure allows for parallel processing at transmit and receive, which is useful to accelerate preparation of the transmitted waveforms and processing of the received signals.

OFDM is a wideband multi-carrier waveform which has the flexibility in the management of its spectrum components. The OFDM spectrum consists of several subcarriers with smaller bandwidth which are orthogonal to each other and separated with a pre-defined frequency spacing of Δf. It is assumed that the OFDM signal generation can be done digitally at a lower frequency band, so that the waveforms can be flexibly designed down to their individual subcarriers and controlled by software to meet the demand of the applications [40]. OFDM subcarriers can be coded for different purposes. In our case, coding the phase of the OFDM subcarriers can be used for reducing the high PAPR of the OFDM signal. If orthogonal codes are given to successive OFDM symbols, it could also provide orthogonality between

the OFDM symbols, which in turn can extend the maximum unambiguous range of the radar. The orthogonalities between OFDM subcarriers and between OFDM symbols allow OFDM radar to produce a range and Doppler profile independent from each other [41]. This is one of the advantages of using OFDM instead of LFM as radar waveform. The above considerations motivate the development of digitally generated beam steering without phase shifter, by providing phase control of the signal directly from waveform generation stage by using OFDM as radar waveform.

As given in (2), adopting the CC scheme produces a beam pattern, essentially like a phased array with phase differences between elements. When multicarrier OFDM signals are transmitted from multiple antennas with a specified time delay difference of Δt, each Δt value produces a beam pattern equivalent to a phased array having inter-element phase difference that depends on the corresponding subcarrier frequencies. Multiple beams can be formed simultaneously, by assigning multiple subcarrier sets which are transmitted using different value of Δt. This idea is the primary contribution of this paper, which will be elaborated in the sequel. A second contribution in this paper concerns the improvement of time on target in a MIMO radar adopting CC-OFDM waveforms. While multiple beamscanning in traditional phased array radar results in limited time on target, CC-OFDM MIMO radar could give a much longer time on target because multiple beams in CC-OFDM radar can be transmitted simultaneously over much longer time intervals.

There are two key problems which may arise from radar transmitting over long continuous time intervals:

- Especially in the case of collocated radar, there will be coupling from the transmit signal to the receiver. This will limit the maximum power that the radar could transmit to avoid saturation problems due to coupling. In a continuous wave (CW) radar system, the transmitter and receiver are always active. Hence, there must be a good isolation between the receiver and transmitter to prevent too high-power coupling of the transmitter output to the receiver input. Therefore, usually CW radar uses a low transmit power levels, which in turn will limit the maximum range of radar detection. In our case, quasi-continuous transmission is used through proper scheduling of OFDM transmission and echoes reception to prevent the coupling.
- The receiver that continuously receives signal echoes coming from multiple targets must be able to distinguish which targets are very near or very far from the radar. This is the reason in this paper that orthogonal codes are given to successive CC-OFDM symbols. These unique codes are given and known by the receiver, so that the receiver could properly detect and distinguish targets nearby and far away from the radar.

In this paper we describe the waveform design of a CC-OFDM quasi-continuous wave for MIMO long range radar. Quasi-CW transmission could limit the leakage/coupling problem by time-isolation of the transmission and reception of the radar system as in a pulse radar system, while it also has the advantage of a CW radar that has a large time bandwidth product. However, the peak-to-average power ratio (PAPR) of OFDM signals becomes an issue because it still may cause too high power-coupling between the array elements. By using a modulation scheme based on OFDM, this will add a stringent requirement on the maximum transmit power per array element to prevent a severe coupling issue between nearby array elements. The high PAPR issue can be solved by using additional phase coding on the OFDM subcarriers. Golay coded OFDM waveform has been claimed to have low PAPR characteristics. Implementing the code to CC-OFDM waveform and transmitting the signals using large arrays makes it possible for CC-OFDM radar to operate at low transmit power. This opens the possibility of using solid-state transmitter for CC-OFDM transmitter modules per array element as can be used in phased array radars.

The proposed CC-OFDM MIMO radar is a combination of CC in MIMO radar and multi carrier OFDM radar to take the advantages of both systems for beamforming at transmit. By using OFDM signal generation, subcarrier allocation for the multiple simultaneous beams can be done in a flexible manner. As will be demonstrated in this paper, it is possible to sparse the total OFDM bandwidth into multiple carrier sets, i.e., sub-bands, responsible for beamforming to the specified direction. Orthogonality between the OFDM subcarriers combined with CC in multiple active antenna systems makes it possible to produce multiple orthogonal beams. When the beams are orthogonal to each other, it is possible that those multiple beams are simultaneously and continuously transmitted to achieve a wide angular coverage at all-time. This means a longer time on target in comparison to the conventional phased array radar, allowing for improved accuracy in target position [22], [42], [43]. Multiple beams of CC-OFDM radar will further allow the application of a monopulse-tracking radar mode, which is beyond the scope of this paper.

Other advantages of using CC-OFDM signal include the multi-dimensional orthogonality, i.e orthogonality in time, subcarrier frequency and space/beam. In this paper, attention is paid to utilizing this multi-dimensional orthogonality. The orthogonality between the CC-OFDM symbols is beneficial in obtaining an optimum SNR for increasing the maximum unambiguous range of the radar. Another main contribution of this paper is the design of a radar waveform which could extend its maximum unambiguous range by transmitting quasi-continuously multiple orthogonal CC-OFDM symbols in series. It means that the radar will have a longer pulse repetition interval (PRI) which leads to a longer-range detection. The additional requirement is that there must be orthogonalities between the symbol series. The orthogonality is provided by using orthogonal codes for coding the CC-OFDM symbols, which can be realized using the Golay codes previously chosen to mitigate PAPR. Moreover, the use of multiple orthogonal OFDM symbols in coherent processing can

improve the Doppler resolution of the radar. Up to this point Golay codes play three important roles in CC-OFDM radar. The codes help to lower the PAPR of the OFDM signals, provide orthogonalities between the beams and achieve the same for the serially transmitted symbols.

B. PRINCIPLE OF CC-OFDM MIMO RADAR

Circulating code in MIMO radar using LFM signals has been implemented for beamforming at transmit [32], [39]. The multiple antenna elements in a linear array with equal element spacing transmit coherent signals having small time-delay difference, Δt, between successive elements. We define Δt_b as a relatively small time-delay difference between successive elements for steering the b-th beam. When coherent signals with delay differences Δt_b are fed to the elements, they will cause phase differences between the elements and so the beam is steered to a certain θ_b direction. Herein, with the transmit antenna index $p = -\frac{N_t-1}{2}, \ldots, \frac{N_t-1}{2}$ and N_t denoting the number of transmit antennas, the transmitted CC-OFDM signal from the p-th transmit antenna element for making the b-th beam can be generally expressed as:

$$x_{b,p}(t) = x(t - p\Delta t_b) \tag{3}$$

By using OFDM signals, the phase differences for beam steering can be added directly to the OFDM subcarrier phases. The role of phase shifters for phase control can be replaced directly by digital WGs operating at frequencies just above a selected low IF. The amplitude control device per T/R module can also be eliminated because it is possible to design a waveform to produce an array pattern with a low sidelobe-level characteristic directly from the waveform generation stage.

This paper describes a novel design of software defined radar (SDR) using CC OFDM waveforms by giving the phase difference for beam steering and the amplitude tapering coefficient at digital waveform generation stage. Hence, when the CC OFDM waveforms are transmitted simultaneously from multiple array antennas, as illustrated in Fig. 1 (a), they will create beams heading to a certain θ_b direction and exhibiting low side lobe levels.

Assume for now that the system is a uniform linear array (ULA) with equal spacing d as depicted in Fig. 1(b). By taking zero reference of θ perpendicular to the array axis, the progressive phase $\psi = kd \sin\theta + \beta$. In OFDM, the wavenumber for the n-th subcarrier at RF:

$$k = \frac{\omega}{c} = \frac{2\pi f_{RF}}{c} = \frac{2\pi(f_n + f_{IF} + f_{up})}{c} \tag{4}$$

where f_n, f_{IF}, f_{up} and f_{RF} denote the baseband frequency f_n of the n-th subcarrier, the intermediate frequency (IF) f_{IF}, the frequency up-conversion shift f_{up} and the radio frequency f_{RF}, respectively, while c is the speed of light.

Let us for now simply assume that the total available bandwidth allocated to the OFDM radar system is divided into sub-bands, each of a given bandwidth, which is a multiple of the subcarrier frequency spacing. Then the phase difference caused by the spacing between adjacent antenna elements becomes:

$$\alpha(\theta) = kd \sin\theta = \frac{2\pi(f_n + f_{IF} + f_{up})}{c} d \sin\theta \tag{5}$$

When the constant phase difference given to the antenna element for steering the beam to θ_b is specified to be $\beta_c = -\alpha(\theta_b)$, then Δt_b can be calculated from:

$$\beta_c(f_{nc,b}, \Delta t_b) = 2\pi f_{nc,b} \Delta t_b = -\alpha(\theta_b) \tag{6}$$

where Δt_b denotes the time delay difference given to the OFDM waveform on the array element for scanning to the b-th beam and $f_{nc,b}$ is the center frequency of the sub-band for beamforming at θ_b. $\beta_c(f_{nc,b}, \Delta t_b)$ defines the phase factor β of the array factor shown in Fig. 1 (b), which is the phase difference between two successive elements at the RF frequency with wavelength λ. The phase factor can also be produced at any p-th transmitter converted to RF. The Taylor amplitude distribution can be applied in the current amplitude I_p on the p-th transmitter to lower the sidelobe level of the beampattern, so that we can define $I'_p = I_p e^{jp2\pi f_{nc,b}\Delta t_b}$.

The array factor (AF) of the CC-OFDM waveform as a function of angle θ, center frequency of the allocated sub band for the b-th beam, $f_{nc,b}$, and time delay Δt_b for phase steering of the b-th beam is given by:

$$\begin{aligned} AF(\theta, f_{nc,b}, \Delta t_b) &= \sum_{p=-\frac{N_t-1}{2}}^{\frac{N_t-1}{2}} I'_p e^{jp\alpha(\theta)} \\ &= \sum_{p=-\frac{N_t-1}{2}}^{\frac{N_t-1}{2}} \underbrace{I_p e^{jp2\pi f_{nc,b}\Delta t_b}}_{\text{the waveform effect}} \underbrace{e^{jp\alpha(\theta)}}_{\text{the array radiation effect}} \end{aligned} \tag{7}$$

The rightmost form consists of the sum of product of two factors. The first represents the waveform effect, which is the Taylor amplitude distribution of the array elements and the phase factor β for beamforming to θ_b. These two parameters are included in the generated OFDM waveform, while the second, the array radiation effect, results from the phase factors α, which is caused by the spacing between the array elements.

For beamforming to an angle of θ_b, the phase difference between successive elements must correspond to the time delay, Δt_b. These multicarrier signals will be circulated with a time shift of Δt_b before being transmitted by the N_t antenna elements in azimuth. When N_b beams are required to cover a given angular range, it means that each of the N_t transmitters will transmit N_b beam signals with their corresponding Δt_b values.

The spectrum division into sub-bands is detailed as follows. Multiple beamforming at transmit is produced by dividing the total OFDM bandwidth B, consisting of N_c subcarriers into N_{sb} sub bands with smaller bandwidth of B_b, consisting of N_{cb} subcarriers. The bandwidth per sub-band B_b will determine the range resolution of the CC-OFDM radar as follows:

$$\Delta R = \frac{c}{2B_b} \tag{8}$$

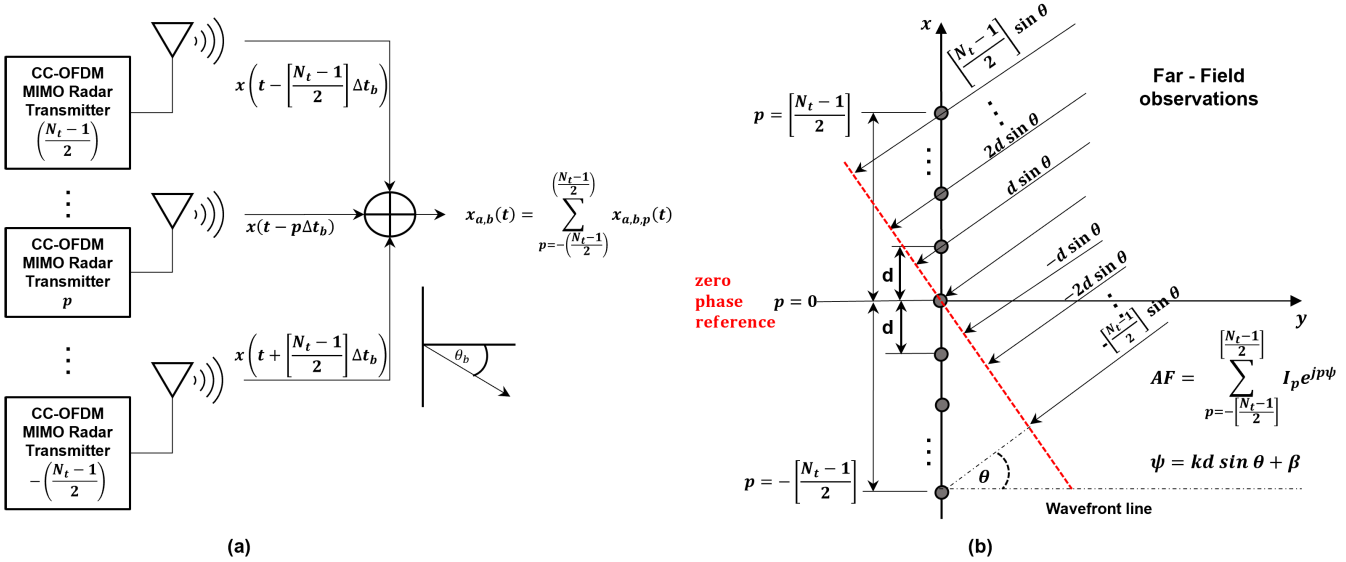

FIGURE 1. Circulating code in OFDM MIMO radar transmitters with N_t elements transmitting coherence signals, delay difference of Δt and array factor is defined in the xy plane: (a) time domain and (b) space domain.

where ΔR is the range resolution in each beam. If the frequency spacing between the OFDM subcarriers are Δf, then the maximum unambiguous range of the OFDM radar is determined by:

$$R_{\mathtt{max\_un}} = \frac{c}{2\Delta f} \tag{9}$$

The total available bandwidth must be used efficiently for multiple beamforming at transmit. Because the bandwidth is limited, it is inevitable that every sub-band must be used for transmitting multiple orthogonal beams. The receiver will be able to distinguish the incoming signals from different beams even when the signals use the same sub-band as long as signals from different beams are coded using orthogonal codes, which once again can be achieved through the use of Golay codes.

In this paper, the sub-band allocation and the beam codes scheduling for the N_b beams are introduced. The schedule is arranged based on the consideration that successive beams do not use the same sub-bands. The same sub-band can be reused for beams which are separated far enough in space. Hence, orthogonality between beams are provided by the Golay codes and the different frequency sub-bands, whereas the large array results in narrow beams and contributes to orthogonality in space domain. To obtain a good PAPR in a sub-band used by multiple beams, it is always attempted to allocate a complementary pair of Golay codes to a pair of beams in the same sub-band.

However, even by using a coded waveform for additional beam orthogonality, assigning an OFDM spectrum consisting of N_{cb} subcarriers to θ_b using a fixed value of Δt_b will cause beam squinting from the lowest subcarrier to the highest subcarrier. This problem can be solved by defining $\beta_c(f_{nc,b}, \Delta t_b)$ as in (6) and implementing CC-OFDM over the full bandwidth while keeping $\beta(f_n, \Delta t)$ constant. To do so, the product of $f_n \Delta t$ must be constant, i.e., when f_n is changing then Δt must also be adapted to make $\beta(f_n, \Delta t)$ constant. The constant value of β is subsequently included into the array factor formula, so that the array factor becomes just a classical phased array factor. The consequence is that there must be a phase correction given to the OFDM code, which means the CC-OFDM waveform must be generated per element. The additional coding for the phase correction is given to the OFDM subcarrier, f_n, transmitted on the p-th element, for all values of p. The relation between the constant phase factor and the phase factor of the n-th OFDM subcarrier can be written as follow:

$$e^{jp2\pi f_n \Delta t_b} = e^{jp\beta_{c,b}} \underbrace{e^{jp(\beta_{n,b}-\beta_{c,b})}}_{\substack{\text{this goes with the} \\ \text{OFDM phase codes}}} \tag{10}$$

where the last phase factor in (10) is the phase correction for the n-th OFDM subcarrier in the p-th transmitter given by:

$$C_{n,p,b} = e^{jp(\beta_{n,b}-\beta_{c,b})} \tag{11}$$

where $\beta_{c,b}$ denotes the constant phase steering of the b-th beam which is defined for the center frequency of the subcarrier sets, and β_n denotes the phase steering of the b-th beam which varies with f_n to make a constant value of $\beta_{c,b}$. the index variable $n = 0, 1, 2, \ldots, N_{c_b} - 1$, denotes the index of the OFDM subcarrier frequency.

An example of application of the CC-OFDM MIMO radar, including the details of the subcarriers and the sub-bands, will be discussed in Section III, but herein we show an example in Fig. 2 of two adjacent beam patterns according to the array factor in (7) coming from a 101-element array antenna with the Taylor amplitude distribution, obtained for a 256-subcarrier OFDM waveform with 10 kHz subcarrier spacings. The beam patterns with solid line are the broadside beams ($b = 0$) which are formed by the 256 subcarriers of

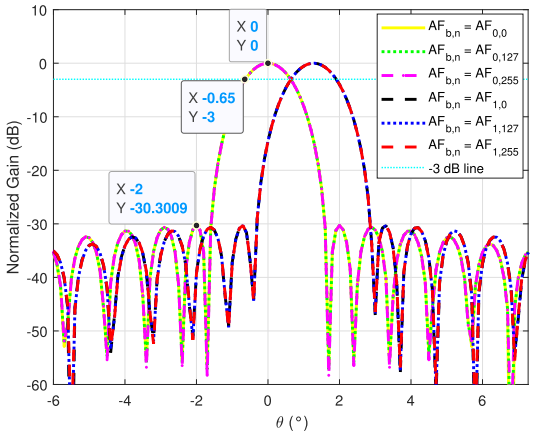

FIGURE 2. Beam pattern of CC-OFDM MIMO radar waveform in the *xy*-plane using 101 elements with Taylor amplitude distribution, and subcarrier frequency spacing of 10 kHz for the broadside beam, $b = 0(\theta_0 = 0°)$, and non-broadside beam, $b = 1(\theta_1 = 1.28°)$ with phase correction given to the OFDM subcarriers.

sub-band 8, occupying a 2.56 MHz bandwidth out of the total available 20.48 MHz. The beampatterns in dotted yellow, green, and magenta are made by the 0-th, 127-th and 255-th subcarriers, respectively, of the 8-th sub band. It can be seen that the three beams coincide with each other, which means that there is no beam squinting caused by the use of multi carrier signal for beam forming. The same occurs for the next adjacent beam, $b = 1$, which refer to $\theta_1 = 1.3°$. This beam is made using a different sub band, that is, 256 subcarriers of sub band 1, to prevent co-channel interference between successive beams. The dotted beampatterns in black, blue and red are the beams made by 0-th, 127-th and 255-th subcarriers of the first sub band, respectively. Again, the beams coincide with each other, since the beam broadening problem has been solved by applying the additional phase corrections to the OFDM subcarriers.

C. TRANSMITTED CC-OFDM RADAR WAVEFORM

The coded baseband OFDM signal of symbol a in beam b which is generated digitally can be defined as:

$$s_{a,b}(k) = \sum_{n=0}^{N_{c_b}-1} g_{a,b,n} e^{j2\pi(n+(z_{a,b}-1)N_{c_b})\Delta f(kT_s-(a-1)T_0)} \quad 0 \le kT_s-(a-1)T_0 \le T_0 \qquad (12)$$

where T_0 is the symbol duration, $a = 1, 2, \ldots, N_{sym}$, beam index $b = [-\frac{N_b-1}{2}, \ldots, 0, \ldots, \frac{N_b-1}{2}]$, $k = [(a-1)n, \ldots, aN_c-1]$ and $z_{a,b}$ denotes the index of the frequency sub-band for the a-th symbol of beam b. N_{sym} symbols are transmitted in series, with time variable $t = kT_s = \frac{k}{f_s}$. The Golay code for the n-th subcarrier for symbol a in beam b is given by $g_{a,b,n}$.

In order to generate CC-OFDM waveform, additional phase steering $\beta(f_{n,a,b}, \Delta t_b)$ is given to the specified OFDM sub-band frequencies of beam b for generating a required time delay between the transmit elements for beam b. The phase steering is defined as:

$$\beta(f_{n,a,b}, \Delta t_b) = 2\pi f_{n,a,b}\Delta t_b \qquad (13)$$

hence, at any transmitter p, the WG generates N_b beams simultaneously during the N_{sym} symbol periods with amplitude control I_p. The CC-OFDM complex signal of symbol a in beam b at the p-th transmitter is:

$$x_{p,a,b}(t) = I_p \sum_{n=0}^{N_{c_b}-1} C_{n,p} g_{a,b,n} e^{jp\beta(f_{n,a,b},\Delta t_b)} \times e^{j2\pi(n+(z_{a,b}-1)N_{c_b})\Delta f(t-(a-1)T_0)} \quad \text{for } 0 \le t-(a-1)T_0+p\Delta t_b \le T_0. \qquad (14)$$

The complex discrete-time signal of the baseband CC-OFDM signal in (14) is:

$$x_{p,a,b}(t) = I_p \sum_{n=0}^{N_{c_b}-1} C_{n,p} g_{a,b,n} e^{jp\beta(f_{n,a,b},\Delta t_b)} \times e^{j2\pi(n+(z_{a,b}-1)N_{c_b})\Delta f(kT_s-(a-1)T_0)} \quad \text{for } 0 \le kT_s-(a-1)T_0+p\Delta t_b \le T_0. \qquad (15)$$

The time delay Δt_b of the OFDM signal must be implemented at the first IF frequency. It could not be implemented in baseband because based on eq (13), regardless of the value of β, the lowest sub carrier frequency of the baseband OFDM signal (f_0) will give undefined result for Δt_b. Hence it is necessary to generate the OFDM signals digitally at the first IF frequency and then implement the time delay at the same digital stage. The digitally generated signals allows for analogue up-conversion the second IF and to the RF frequency band. The first digital IF frequency must be low enough, because the higher the frequency would give the lower value of Δt. For instance, when an IF frequency of 10 MHz is used, the Δt value is already in the order of nanoseconds. Hence it will cause a strict requirement on the stability and the precision of the oscillator clocks of the WG. Moreover, the waveforms are generated individually by the transmitters, which means all N_t WGs must be phase-locked to the same external clock so that the transmit signals will have the correct phase difference between the transmit elements for beamforming to the specified direction. This is necessary because OFDM signal is susceptible to Carrier Frequency Offset (CFO). CFOs in OFDM MIMO radar are caused by the Doppler frequency of moving targets and by the hardware CFO. When there is misalignment of the OFDM subcarriers, it will affect the accuracy of radar detection.

The same requirement yields for the up/down conversion oscillator, as well as for the N_t oscillator clocks at each transmit and receive modules. They must be also phase-locked to the same external clock. It is necessary to avoid the CFO problem caused by a mismatch of the digital clocks in the transmitter and receiver since it will cause sampling frequency offset (SFO) and may affect the phase correction $e^{jp(\beta_n-\beta_c)}$ in (11). The CFO and SFO should be kept very small, because otherwise it may cause false radar detection.This leads to a

strict requirement for the time and frequency accuracy of the oscillator clocks at transmitters and receivers. For instance, with an IF of 20 MHz and a carrier frequency offset of 10 kHz the error in beam direction becomes 0.1° and the estimated range error equals 0.27 meter for a target at the maximum range of 180 km.

Based on above considerations the baseband CC-OFDM waveform in (15) should be digitally up-converted to the first IF, hence the signal will be in the spectrum of f_{IF} to $f_{IF} + B$. Accordingly, the CC-OFDM signal at the first IF stage, $x^{IF}_{p,a,b}(k)$, in (15) is generated digitally by the WG at transmitter p. It means that each WG generates N_{sym} symbols for the N_b beams with an amplitude control of I_p. By including the amplitude control coefficient I_p and phase steering to the OFDM waveform, the CC-OFDM waveform at the first digital IF stage becomes:

$$x^{IF}_{p,a,b}(k) = I_p \sum_{n=0}^{Nc_b-1} C_{n,p,a,b} g_{a,b,n} e^{jp\beta(f_{n,a,b},\Delta t_b)} \times e^{j2\pi(\frac{f_{IF}}{\Delta f}+n+(z_{a,b}-1)N_{c_b}\Delta f(kT_s^{IF}-(a-1)T_0)} \quad \text{for } 0 \le kT_s^{IF} - (a-1)T_0 + p\Delta t_b \le T_0. \quad (16)$$

By substituting (13) into (16), the digital IF waveform becomes:

$$x^{IF}_{p,a,b}(k) = I_p \sum_{n=0}^{Nc_b-1} C_{n,p,a,b} g_{a,b,n} \times e^{j2\pi(\frac{f_{IF}}{\Delta f}+n+(z_{a,b}-1)N_{c_b}\Delta f(kT_s^{IF}-(a-1)T_0+p\Delta t_b)} \quad \text{for } 0 \le kT_s^{IF} - (a-1)T_0 + p\Delta t_b \le T_0. \quad (17)$$

III. AN EXAMPLE OF CC-OFDM MIMO RADAR FOR LONG-RANGE SURVEILLANCE

A. REQUIREMENTS

To elucidate the novel concept and detailed implementation of the CC-OFDM MIMO radar, we will take a surveillance radar design as an example for analyses in the subsequent sections. The CC-OFDM MIMO radar waveform designed herein is based on the requirement of surveillance radars used in coastal areas, where the target of interest are ships and small aircrafts in the area within 180 km from the radar site. OFDM signals with subcarrier spacing of 10 KHz will give a maximum unambiguous range of 15 km. In order to extend the maximum unambiguous range of the radar up to 180 km, 12 orthogonal OFDM symbols with symbol time of 0.1 ms are transmitted in series. The 12 OFDM signals are transmitted in quasi-continuous way, since the transmitter is idle during the reception period within one repetition time interval. The CC-OFDM MIMO radar system and waveform specifications are described in Table 1 In this case, each sub band which consists of 256 subcarriers are used for beamforming; that leads to 2.56 MHz bandwidth and results in a range resolution of 60 meters in each beam. The OFDM signal period is 0.1 ms and the spacing between subcarriers is $1/T$ (i.e., 10 kHz). A surveillance radar requires a pencil

TABLE 1. Surveillance radar system and waveform specifications.

Radar Specification:		Units
Carrier Frequency	3	GHz
Bandwidth	20.48	MHz
Antenna Beamwidth (Azimuth)	< 2	Degree
Antenna Beamwidth (Elevation)	20	Degree
Antenna Gain	34	dBi
Maximum Sidelobe Level (SLL)	-26	dB
Transmit power per T/R Module	10-50	mW
Noise Figure	<6	dB
Min SNR	12	dB
Dynamic Range	70	dB
Maximum Doppler Frequency	1	kHz
Range Resolution	60	meter
Maximum range	180	Km
Minimum RCS Minimum average power per element	100 4.7	m^2 mW

Waveform Specification:		Units
OFDM symbol duration	0.1	ms
Number of symbols/frame	12	Symbols
PRI	1.2	ms
Extra repetition interval	3.2	ms
Number of T/R modules	101	Modules
Number of frames	16	Frames
Number of sub bands	8	Sub bands
Number of sub carrier/sub band	256	Sub carriers
Number of beams for scanning from $-45°$ to $45°$	63	Beams
Amplitude tapering using Taylor for SLL	-30	dB

beam with a beamwidth of less than 2° in the azimuth plane. The azimuth and elevation beamwidth requirements of less than 2° and 20°, respectively, can be obtained with a planar array of 101 elements in the azimuth and 21 elements in elevation, which leads to a gain of 33 dB assuming isotropic elements and no amplitude taper. The 21-element structure can be realized as a vertical array, instead of a single element that is a part of the horizontal linear array previously assumed, attached to each transmitter. Fig. 3(a) shows the azimuth beampatterns of the 101-element linear array with uniform amplitude distribution (as shown in Fig. 3(c)) and with −30dB Taylor amplitude tapering; the beampattern of the ULA with a uniform amplitude tapering has a 3dB beamwidth of 1°, while the Taylor one has a beamwidth of 1.3° and all sidelobes of the array with Taylor tapering are below −30 dB. In order to find the number of beams, it is necessary to define the main beams direction, θ_c, subject to the condition that successive beams must overlap at their 3-dB points. The procedure in finding the number of beams required for fulfilling the mission requirement is done as given in the following:

1) The first beam will be the broadside beam $\theta_c(0) = 0$. According to Fig. 3, the first upper 3dB point is at

0.64 deg. Because the beam is symmetrical around the center mainlobe, θ_c, the first lower 3dB point value is $-0.64°$.

2) The next mainlobe θ_c (1) can be found using the following expression:

$$\theta_c(1) = \theta_{3\text{dB},0} + \frac{\theta_{3\text{dB},0}}{\cos\theta_{3\text{dB},0}} \tag{18}$$

The second term in (18) is for finding the next θ_c value which also considers the beamscanning loss as a function of $\frac{1}{\cos\theta_c}$.

3) The next beam, $b = 2$, will have a main beam which is at:

$$\theta_c(2) = \theta_{3\text{dB},0} + 2\theta_{3\text{dB},1} + \frac{\theta_{3\text{dB},1}}{\cos(\theta_{3\text{dB},0} + 2\theta_{3\text{dB},1})} \tag{19}$$

The second term in (19) is actually the 3-dB beamwidth of beam 1.

4) For any beam, $b = \ell$, the maximum of the beam is at:

$$\begin{aligned}\theta_c(\ell) &= \theta_{3\text{dB},0} + 2\theta_{3\text{dB},1} + \cdots + 2\theta_{3\text{dB},\ell-1} \\ &\quad + \frac{\theta_{3\text{dB},\ell-1}}{\cos(\theta_{3\text{dB},0} + 2\theta_{3\text{dB},1} + \cdots + 2\theta_{3\text{dB},\ell-1})} \\ &= \theta_{3\text{dB},0} + 2\sum_{l=1}^{\ell-1}(\theta_{3\text{dB},l} \\ &\quad + \frac{\theta_{3\text{dB},\ell-1}}{\cos(\theta_{3\text{dB},0} + 2\sum_{l=1}^{\ell-1}\theta_{3\text{dB},l})})\end{aligned} \tag{20}$$

Step 4 is repeated until the last beam reaches 45° angle.

If elements with a generic pattern of $\cos(\theta)$, instead of isotropic elements, are considered, additional 7 dB to the gain leads to 40 dBi at broadside. However, for the same reason, when $\cos(\theta)$ element is used, a loss of 3 dB occurs at 45° scan angle. Additional loss due to scanning known as scan loss, when the radar is scanning to 45°, is $1/\cos(45°) = 1.5$ dB. This gives the antenna gain of the 101×21 elements array for surveillance at maximum scan angle around 35.5 dBi. It can be seen from Fig. 3(a), the tapering loss caused by Taylor amplitude tapering is around 1.1 dB, hence the antenna gain at the maximum scan angle becomes 34.4 dB. For the surveillance radar specifications as given in Table 1, 10 kHz receiver processing bandwidth is found per symbol time; if 12 symbols are transmitted serially and repeated 32 times for coherent Doppler processing, the receiver bandwidth after Doppler processing will become $\frac{10\times10^3}{(12)(32)} = 26$ Hz. Related to the mission requirement, the required maximum unambiguous range is 180 km. With a receiver noise figure $F_n = 4$ (6 dB) and minimum signal to noise ratio $SNR_{min} = 16$ (12 dB) the minimum received power after post Doppler processing is given by σ,

$$S_{min} = kTF_nSNR_{min}\text{B}_{\text{postDoppler}} \tag{21}$$

where k is Boltzmann's constant, T is the absolute temperature (K). Substituting $F_n = 4$ and $SNR_{min} = 16$ into eq (21)

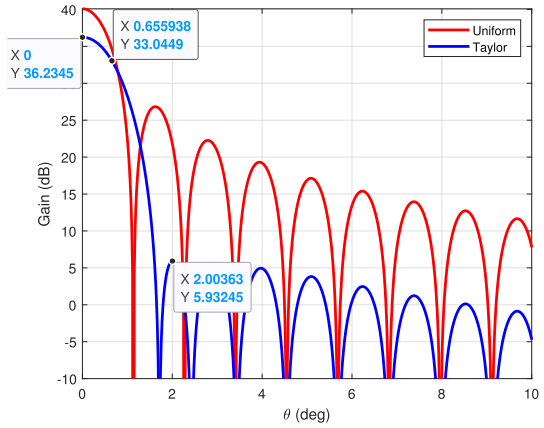

(a)

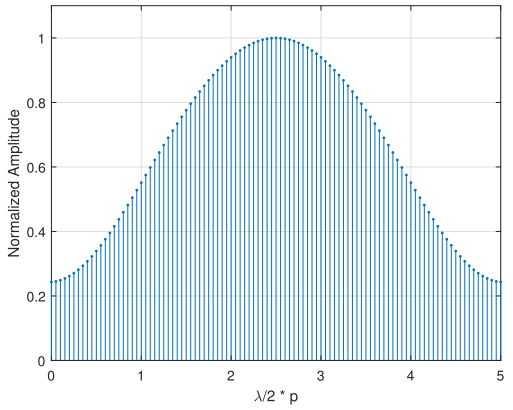

(b)

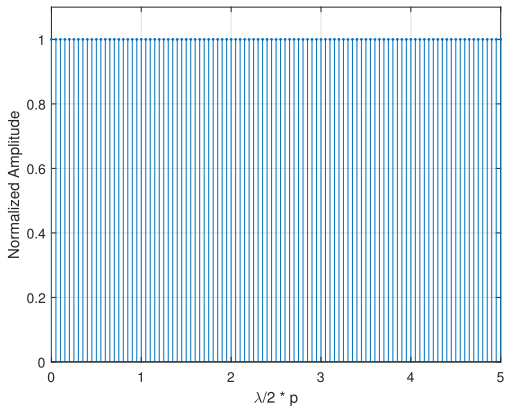

(c)

FIGURE 3. (a) Beampattern of 101 ULA with uniform and taylor amplitude tapering, (b) uniform, (c) Taylor amplitude tapering coefficient for 101 ULA.

gives $= 6.67 \times 10^{-18}$ Watt. The minimum average transmit power for detecting a target with RCS is given by

$$P_{av} = \frac{(4\pi)^3R^4S_{min}}{G_tG_r\lambda^2\sigma} \tag{22}$$

Substituting in (22) $R = 180$ km, $S_{min} = 6.67 \times 10^{-18}$ Watt, the transmit antenna gain G_t = receive antenna gain G_r = 2754(34.4dBi), $\lambda = 0.1$ m and $\sigma = 100$ m^2 the

minimum average transmit power for a single beam transmission becomes 1.83 Watts and for a 101 × 21 planar array the minimum average power per element will be around 0.86 mW. Using the same parameters and calculating for the minimum RCS, $\sigma = 1$ m^2, the minimum average transmit power becomes 100 times higher, which result in 86 mW per element.

Considering simultaneously transmitting 63 beams of CC-OFDM signals, the transmit power requirement of the CC-OFDM MIMO surveillance radar may increase, because the PAPR values of the transmitted signal must be taken into consideration as well. The detailed PAPR analysis of CC-OFDM signal will be discussed in Section IV-A. Table 3 shows that the maximum PAPR value for transmitting 63 beams CC-OFDM over a symbol period of 0.1ms is 7.4 dB (= 5.5). As a consequence, the average power of transmitting 63 beams simultaneously will be 5.5 times higher. Hence the transmit power per element for a minimum RCS $\sigma =$ 100 m^2 and 1 m^2 at a maximum range of 180 km equals to 4.7 mW and 470 mW respectively. Due to antenna element coupling and CW transmission at short ranges the maximum power per element is limited in order to avoid receiver saturation. The maximum transmit power should not be higher than 50 mW per element. The proposed radar design can fulfill the requirement for minimum RCS of 100 m^2 at the maximum range of 180 km. In order to have a higher sensitivity at the maximum range, it is possible to make the radar to operate in low power mode for short range detection and high-power mode for the long-range radar. The low-power mode with the minimum RCS of 100 m^2 is given in this paper, while for the long-range radar with higher sensitivity is described in a separate paper.

B. SURVEILLANCE CC OFDM RADAR SYSTEM

CC OFDM transmitter and receiver block diagram in Fig. 4 consists of simple transmit and receive modules. The transmit module consist of CC OFDM digital WG which generates OFDM signal at the first digital IF frequency and implementation of the time delay for beamforming. The digital IF signal goes through the digital-to-analog converter, then the analogue signal goes through the transmitter chain, which consists of the IF and RF analogue up-converters and power amplifier (PA). The output of the PA then goes to power divider and then the signal is distributed to 21 vertical elements. The combined transmit signal from 101 transmitters will create 63 beams simultaneously that are transmitted in quasi-continuously manners to prevent leakage. Meanwhile, when the target echo is received by the antenna subsystem, the signals received on the 21 vertical antennas are combined. Then the received RF signal goes through the analog receiver chain, which consist of LNA and the RF to IF down-converters. Then the first IF analog signal is converted into digital through an analog-to-digital converter, and it is processed furthermore by radar digital signal processor (DSP) to get information on the target profiles.

Analogue filters shown in Fig. 4 are implemented in between the up-converter steps at transmitter as well as in between the down converter steps at the receiver to get rid of the signal harmonics. As explained in Section 1B, The CC-OFDM waveform must be generated at each antenna element because the generated signal contains the amplitude control and phase correction per element needed for lowering the sidelobe of the resulting beampattern and compensating the beam broadening effect, respectively. The 63 beam signals are transmitted simultaneously from 101 azimuth antenna elements, and the 101 digital WGs and DSPs are phase-locked to the same external clock.

As the consequence of compensating the beam broadening issue described previously, it can be seen from (11) that the phase correction, $C_{n,p,a,b}$ is given to the n-th subcarrier frequency of the OFDM waveform generated for the p-th transmitter for beamforming to θ_b of symbol a. The Taylor coefficient for sidelobe suppression I_p in (7) is also digitally generated directly from the WG. It is for these two reasons that the CC-OFDM waveforms must be generated simultaneously per row of the azimuth antenna elements. It is therefore necessary to implement a digital WG at each transmitter with programmability feature, since different radar applications might require different parameters for the beams, waveforms, symbols and frames of symbols. Consequently, the adoption of the concept of software-defined radar (SDR) platform is advantageous and instrumental in the CC-OFDM MIMO radar, promotes the flexibility of the radar and opens up various possibilities of design applications.

Using the long-range surveillance radar introduced in Section III as reference, Fig. 5 shows the detailed procedure of CC-OFDM digital WG and coding block in Fig. 4. The Golay code generator programmed in the SDR generates 256 Golay codes, consisting of 128 complementary pair codes. A unique Golay code with a code length of 256 bits is used because in this paper, 256 successive subcarriers are grouped into one sub-band and transmitted through one beam. The codes are used for coding the 63 beams using 8 available sub-bands. A certain combination of the Golay codes for the beam and for the symbol must be chosen in order to provide orthogonality between beams and between symbols while at the same time keeping PAPR low. The codes are assigned to the subcarriers according to the transmission schedule, while ensuring that there are no successive beams that use the same sub-band and all the beams are coded using unique codes.

For better understanding on how the signal transmitted through a beam is generated, Fig. 5 shows an example when one beam signal (i.e., beam −31) is generated using sub-band 1 and coded with Golay code, $g_{1,-31}$, while subcarriers in the other sub-bands are set to zero. The Golay code is applied in the frequency domain of the OFDM signal and then the signal is phase shifted by $p\beta(f_{n,a,b}, \Delta t_b)$, with $p = -50, -49, \ldots, 0, \ldots, 49, 50$, since the zero phase-reference is at the centre of the array. The phase steering is also given in the frequency domain of the OFDM signal generated for the p-th transmitter. The phase steering is infused in the

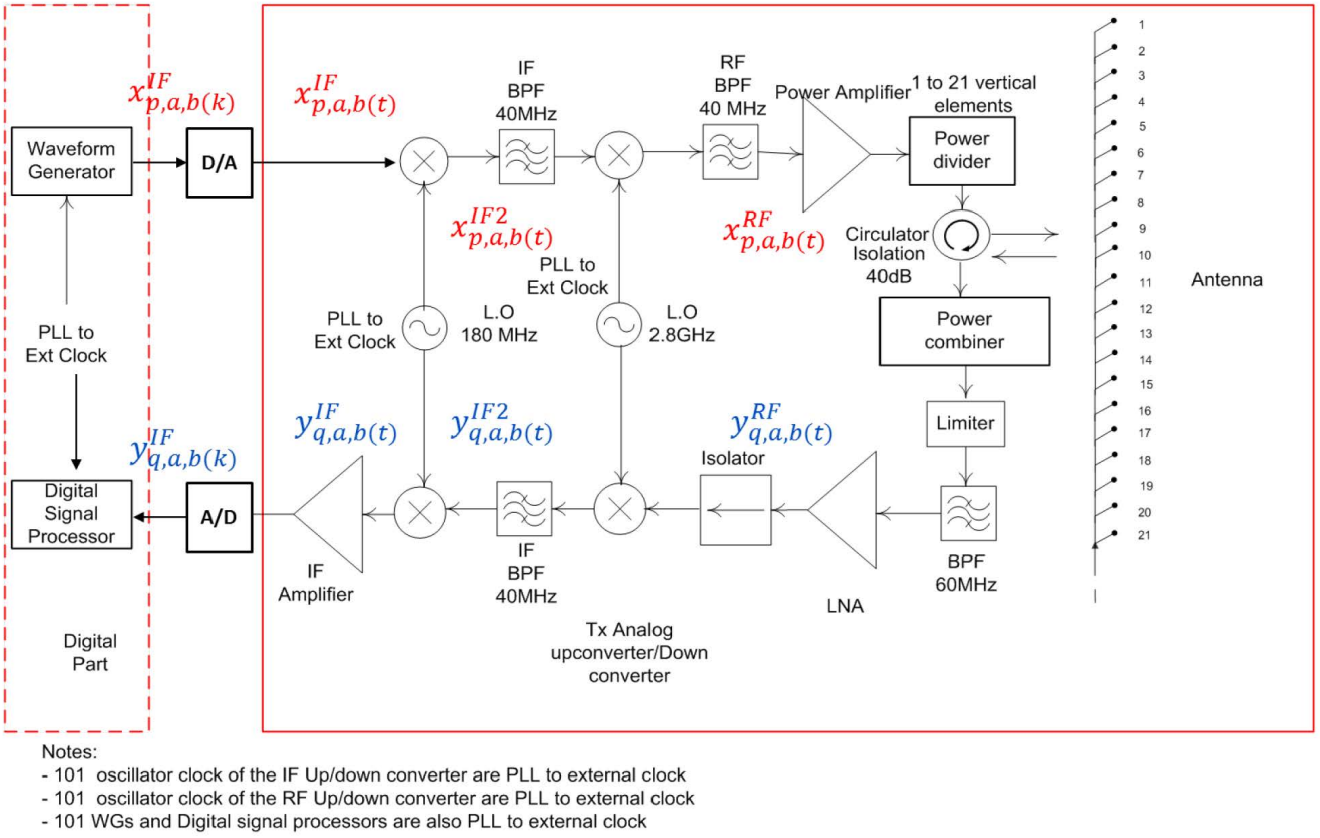

FIGURE 4. Block diagram of a T-R module of CC-OFDM MIMO radar system.

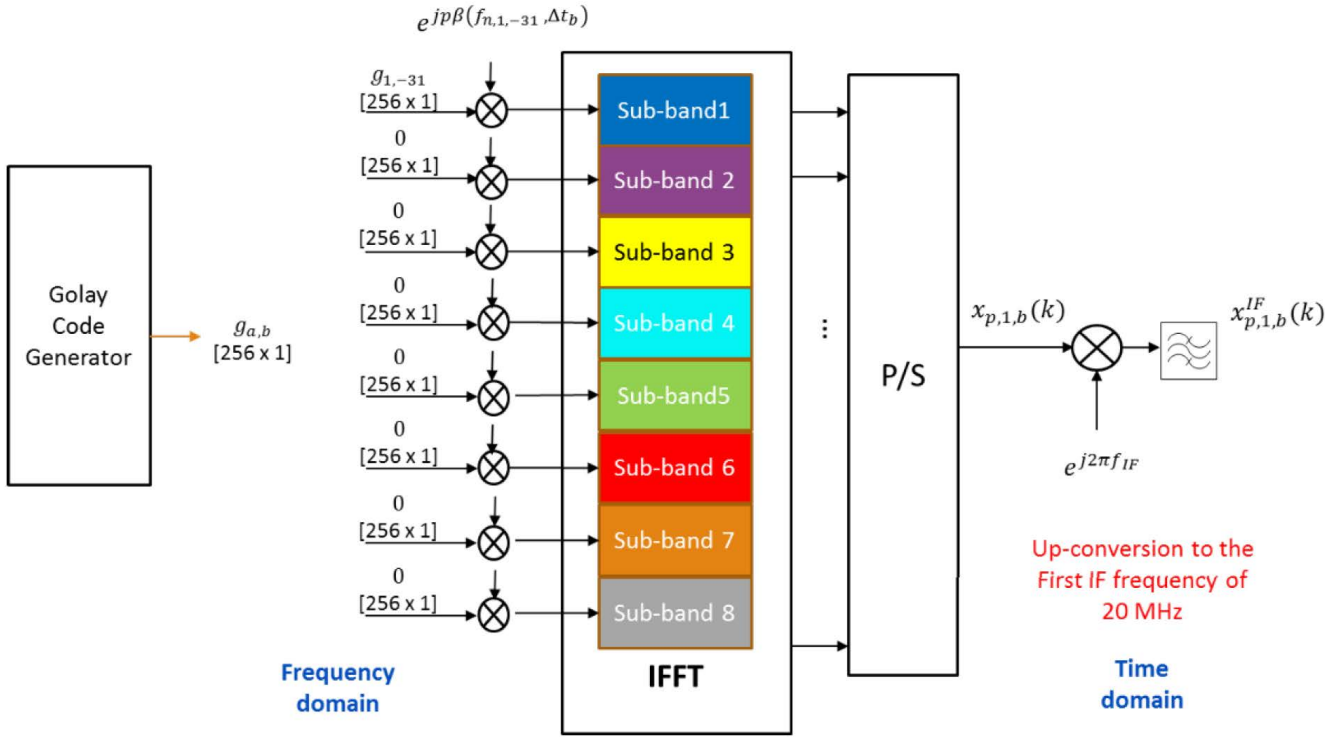

FIGURE 5. CC-OFDM digital WG and coding for symbol 1 in beam $b = -31$ on the p-th transmitter, which also involves digital up-conversion from baseband to the first IF. Each sub-band consists of 256 subcarriers.

OFDM signal by multiplying the coded OFDM signal with $e^{jp\beta(f_{n,a,b},\Delta t_b)}$. The coded CC-OFDM signal can be obtained by taking the IFFT of the whole 8 sub-band (consisting of 2048 sub carrier frequencies). Subsequently, the signal is digitally up converted to the first IF frequency, $x^{IF}_{p,a,b}$. After digital up-conversion, the IF signal output of the WG, $x^{IF}_{p,a,b}$, will be converted to analog signals through a DAC device of the p-th transmitter. Using the same procedure, the 63 beam signals are generated simultaneously by the digital WG at each transmit element.

For a good operational performance of CC OFDM MIMO radar an important and crucial note should be made now, that is: Transmitting multiple symbols in series and in parallel contributing simultaneously to multiple beams effective in various range intervals, the quasi - CW transmission necessitates that the CC OFDM symbols should be orthogonal in time, frequency and code. In the following the orthogonality aspects are detailed.

- Single CC OFDM symbol
  In this example, one symbol of CC-OFDM waveform contributes to 63 beam signals. The 63 beam signals are carried by a limited number of sub-bands. Hence it is crucial to have a unique Golay code for each of the 63 beams. In the surveillance radar design, there are only 8 sub-bands available and, hence, each sub-band is transmitting 7 to 8 beams at the same time.
- Multiple CC OFDM symbols
  The orthogonality between symbols is provided by different Golay codes for the 12 symbols transmitted in beam b. Since the number of Golay codes are limited (there are in total 256 available Golay codes that can be used for 256-subcarrier OFDM symbols), code reuse becomes inevitable. According to the mission requirement specified in Table 1, as many as 12×63 codes are required for providing orthogonality between symbols and between beams, while there are only 256 codes available. Therefore, the codes need to be reused at least 3 times. In order to maintain the orthogonality, the 12 symbols transmitted in each beam must be transmitted using 3 different sub-bands. Consequently, code scheduling for the beams and for the symbols must ensure that there should be no code reuse for different beams in the same CC-OFDM symbol, and there is no code reuse for different symbols of the same beams. Table 2 shows the transmit scheduling of $x_{a,b}$, which is the transmit CC-OFDM symbol a of beam b. For a certain beam b, there are 12 symbols ($a = 1, 2, \ldots, 12$) which are coded using certain unique Golay codes and occupying 3 (out of 8) different sub bands. The 8 colors illustrate the sub band allocation of the beam. The number in the colored rectangles show the index of the Golay code use by the beam. It can be seen from Table 2, that the pattern of the sub band allocation is repeated every 8 consecutive beams. The sub band combination for beam -31 to beam -24 can be reused in beam -23 to beam -16, and the reused again in beam -15 to -8 and so on. It means that there will be a co-channel beam with 8 beams in between. For these co-channel beams, the orthogonalities will rely on the orthogonality of the Golay codes and the fact that the two nearest co-channel beams will have an angular space of ± 10 degrees in between. The sub band combination can be repeated every 8 beams, however, Golay code repetition is only permitted for a different beam in a different symbol which are using a different sub band. It can be seen in Table 2, for the transmit scheduling of beams -31 to -24, each beam has a different sub-band combinations and a different Golay codes for a specific beam of the same symbol. However, there are some codes repetitions on the scheme, for example the code repetition of the first Golay code in the transmit schedule of beam -31, -29 and beam -26, in symbol 1, 5 and 9 respectively. The three beams are using the same Golay code in different symbol. This is allowed because the three beams are transmitted using a different sub band combinations. Hence the orthogonalities between the transmitted beams still can be maintained.

The IF coded CC-OFDM symbol, $x^{IF}_{a,b}(t)$, is frequency shifted by analogue up-conversion from 20 MHz to the second IF frequency of 200 Mhz, with $f_{IF2} = 180$ MHz:

$$x^{IF2}_{p,a,b}(t) = x^{IF}_{p,a,b}(t)\, e^{j2\pi f_{IF2} t} * h_{IF2}(t) \tag{23}$$

Furthermore, up-conversion of the second IF signal in (23) to the RF frequency band of 3 GHz is realized via

$$x^{RF}_{p,a,b}(t) = x^{IF2}_{p,a,b}(t)\, e^{j2\pi f_{RF} t} * h_{RF}(t) \tag{24}$$

where $f_{RF} = 3GHz - f_{IF2} - f_{IF}$, while $h_{IF2}(t)$ and $h_{RF}(t)$ denote the impulse responses of the filters used to suppress the unwanted frequencies (product terms) at the second IF and RF frequencies, respectively, with $*$ denoting the convolution operator. As an example, for the ideal filter at the second IF the frequency response can be in the form of:

$$|H_{IF2}(f)| = \begin{cases} 1, & 200 \le f \le 220.48\text{MHz} \\ 0, & \text{elsewhere} \end{cases} \tag{25}$$

And the frequency response of the ideal BPF at RF frequency will be:

$$|H_{RF}(f)| = \begin{cases} 1, & 3000 \le f \le 3020.48\text{MHz} \\ 0, & \text{elsewhere} \end{cases} \tag{26}$$

After up-conversion, the signal is transmitted through the transmit element p. Because we have applied the additional phase steering, the analog signal aggregate which is the combining of the transmit signal from 101 element will steer the beam to a specified beam b.

The 101 transmitters transmit their respective signals coherently, each signal having been infused with the additional phase steering, $\beta(f_{n,a,b}, \Delta t_b)$, and amplitude tapering coefficient in the waveform. As a result, when these signals

TABLE 2. Transmit scheduling of multi-beam CC-OFDM MIMO radar with taylor amplitude tapering = −30 dB which includes the sub band and golay codes allocation per beams for 12 Symbols of beam −31 to beam 31.

Repeat the sub band allocation pattern every 8 consecutive beams

$\theta_b(°)$	b	Symbol											
		1	2	3	4	5	6	7	8	9	10	11	12
-43.1	-31	1	33	65	97	13	45	77	109	125	29	61	93
-41.5	-30	9	41	73	105	21	53	85	117	5	37	69	101
-39.8	-29	17	49	81	113	1	33	65	97	13	45	77	109
-38.2	-28	25	57	89	121	9	41	73	105	21	53	85	117
-36.6	-27	5	37	69	101	17	49	81	113	121	25	57	89
-35.1	-26	13	45	77	109	25	57	89	121	1	33	65	97
-33.6	-25	21	53	85	117	125	29	61	93	9	41	73	105
-32.1	-24	29	61	93	125	5	37	69	101	17	49	81	113
-30.6	-23	129	161	193	225	141	173	205	237	253	157	189	221
-29.2	-22	137	169	201	233	149	181	213	245	133	165	197	229
-27.7	-21	145	177	209	241	129	161	193	225	141	173	205	237
-26.3	-20	153	185	217	249	137	169	201	233	149	181	213	245
-24.9	-19	133	165	197	229	145	177	209	241	249	153	185	217
-23.5	-18	141	173	205	237	153	185	217	249	129	161	193	225
-22.2	-17	149	181	213	245	253	157	189	221	137	169	201	233
-20.8	-16	157	189	221	253	133	165	197	229	145	177	209	241
-19.4	-15	2	34	66	98	14	46	78	110	126	30	62	94
-18.1	-14	10	42	74	106	22	54	86	118	6	38	70	102
-16.8	-13	18	50	82	114	2	34	66	98	14	46	78	110
-15.5	-12	26	58	90	122	10	42	74	106	22	54	86	118
-14.1	-11	6	38	70	102	18	50	82	114	122	26	58	90
-12.8	-10	14	46	78	110	26	58	90	122	2	34	66	98
-11.5	-9	22	54	86	118	126	30	62	94	10	42	74	106
-10.2	-8	30	62	94	126	6	38	70	102	18	50	82	114
-9	-7	130	162	194	226	142	174	206	238	254	158	190	222
-7.7	-6	138	170	202	234	150	182	214	246	134	166	198	230
-6.4	-5	146	178	210	242	130	162	194	226	142	174	206	238
-5.1	-4	154	186	218	250	138	170	202	234	150	182	214	246
-3.8	-3	134	166	198	230	146	178	210	242	250	154	186	218
-2.6	-2	142	174	206	238	154	186	218	250	130	162	194	226
-1.3	-1	150	182	214	246	254	158	190	222	138	170	202	234
0	0	158	190	222	254	134	166	198	230	146	178	210	242
1.3	1	3	35	67	99	15	47	79	111	127	31	63	95
2.6	2	11	43	75	107	23	55	87	119	7	39	71	103
3.8	3	19	51	83	115	3	35	67	99	15	47	79	111
5.1	4	27	59	91	123	11	43	75	107	23	55	87	119
6.4	5	7	39	71	103	19	51	83	115	123	27	59	91
7.7	6	15	47	79	111	27	59	91	123	3	35	67	99
9	7	23	55	87	119	127	31	63	95	11	43	75	107
10.2	8	31	63	95	127	7	39	71	103	19	51	83	115
11.5	9	131	163	195	227	143	175	207	239	255	159	191	223
12.8	10	139	171	203	235	151	183	215	247	135	167	199	231
14.1	11	147	179	211	243	131	163	195	227	143	175	207	239
15.5	12	155	187	219	251	139	171	203	235	151	183	215	247
16.8	13	135	167	199	231	147	179	211	243	251	155	187	219
18.1	14	143	175	207	239	155	187	219	251	131	163	195	227
19.4	15	151	183	215	247	255	159	191	223	139	171	203	235
20.8	16	159	191	223	255	135	167	199	231	147	179	211	243
22.2	17	4	36	68	100	16	48	80	112	128	32	64	96
23.5	18	12	44	76	108	24	56	88	120	8	40	72	104
24.9	19	20	52	84	116	4	36	68	100	16	48	80	112
26.3	20	28	60	92	124	12	44	76	108	24	56	88	120
27.7	21	8	40	72	104	20	52	84	116	124	28	60	92
29.2	22	16	48	80	112	28	60	92	124	4	36	68	100
30.6	23	24	56	88	120	128	32	64	96	12	44	76	108
32.1	24	32	64	96	128	8	40	72	104	20	52	84	116
33.6	25	132	164	196	228	144	176	208	240	256	160	192	224
35.1	26	140	172	204	236	152	184	216	248	136	168	200	232
36.6	27	148	180	212	244	132	164	196	228	144	176	208	240
38.2	28	156	188	220	252	140	172	204	236	152	184	216	248
39.8	29	136	168	200	232	148	180	212	244	252	156	188	220
41.5	30	144	176	208	240	156	188	220	252	132	164	196	228
43.1	31	152	184	216	248	256	160	192	224	140	172	204	236

Sub band 1
Sub band 2
Sub band 3
Sub band 4
Sub band 5
Sub band 6
Sub band 7
Sub band 8

are radiated by the corresponding 101 antennas, multiple beams are formed, with every beam b is being steered to a certain angle θ_b.

IV. MULTI BEAM ARRAY PATTERN AT TRANSMIT

This section describes the design procedure for making multiple beams of the CC-OFDM radar waveform using multiple

sub band frequencies. Successive beam patterns are made to have a crossover at their respective 3 dB points to provide radar with the possibility of applying a mono-pulse tracking radar mode. The design steps of the multiple beams can be described as follows:

i. Define the required number of beams N_b by invoking the procedure given in Section III-A.
ii. Determine the time delay Δt_b which corresponds to the phase steering of the b-th beam to get the wanted angular scanned resolution. First the time delay for phase steering, Δt_b, is defined for the broadside beam ($\theta_0 = 0°$) and is equal to zero ($\Delta t_0 = 0$). The special case for the broadside beam means that the beam is independent to the subcarrier frequency, because $\Delta t_0 = 0$ whichever sub band frequency is assigned for it.
iii. Determine the bandwidth and subcarrier frequencies set which are allocated for the broadside beam, $b = 0$. It is arranged so that for successive beams the same band allocation will not be used.
iv. Get the beam pattern $AF_b(\theta, f_n, \Delta t_0)$ of the broadside beam
v. Calculate the Δt_b for the next beam b, by using a different sub band frequency than the sub band used by the previous beam, $b - 1$. In this paper, the time delay Δt_b will be calculated by using the center frequency of the allocated sub band which already was described in the transmitter schedule in Section 2.
vi. Get the beam pattern $AF_b(\theta, f_{n,b}, \Delta t_b)$ of beam b.
vii. Repeat step v and vi for the next beam $b \leftarrow b + 1$ until the required number of beams is fulfilled.

V. PEAK TO AVERAGE POWER RATIO

A potential negative issue of high PAPR value is caused by using simultaneously OFDM waveforms. In this paper, Golay code for phase coding the OFDM subcarrier is used for lowering the PAPR of the OFDM signal. Lowering the PAPR value can be obtained by arranging the code allocation and properly choose Golay complementary pairs for coding the beams which are using the same sub band. In this paper, the PAPR analysis of multiple beam CC OFDM waveforms which are transmitted using 8 sub bands will be discussed.

Recall the formulation of the b-th beam transmitted from the center array in (16) which define the a-th CC OFDM symbol, transmitted by the p-th transmit antenna as $x_{p,a,b}(k)$. The PAPR of the transmitted symbol a of beam b from the p-th transmitter can be calculated as follows:

$$\mathrm{PAPR}_{p,a,b}(\mathrm{dB}) = 10\log\left[\frac{\max\left[x_{p,a,b}(k)\, x^*_{p,a,b}(k)\right]}{\mathrm{E}\left[x_{p,a,b}(k)\, x^*_{p,a,b}(k)\right]}\right] \tag{27}$$

The simulation result shows that the PAPR per beam of symbol a at the p -th transmit element is around 3 dB. While the PAPR of the total transmitted beams can be obtained by

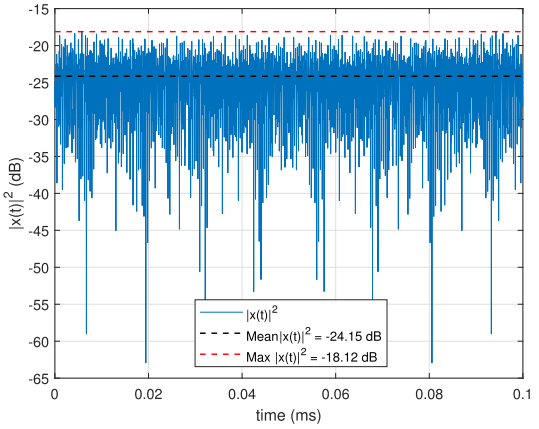

(a)

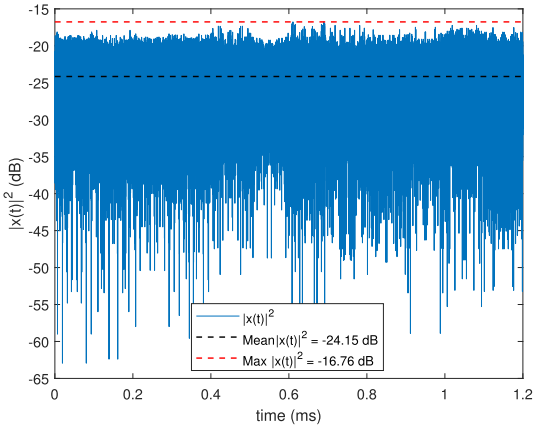

(b)

FIGURE 6. The instantaneous power of 63 beams CC-OFDM signals transmitted from transmitter $p = 0$: (a) over 12 successive symbols period and (b) over one symbol period.

summing up the 63 beam signals power as follows:

$$\mathrm{PAPR}_{p,a}(\mathrm{dB}) = 10\log\left[\frac{\max\left[\sum_b x_{p,a,b}(k)\, x^*_{p,a,b}(k)\right]}{\mathrm{E}\left[\sum_b x_{p,a,b}(k)\, x^*_{p,a,b}(k)\right]}\right], \quad 0 \le kT_s - (a-1)T_0 + p\Delta t_b \le T_0 \tag{28}$$

Assuming that there are no CFO and SFO in the transmitter chain, the PAPR will depend on the amplitude tapering coefficient and the Golay codes as given by:

$$\mathrm{PAPR}_{p,a}(\mathrm{dB}) = 10\log\left[\frac{\max\left[I_p I_p^* \sum_b \sum_{n=0}^{N_c-1} g_{a,b,n} g^*_{a,b,n}\right]}{\mathrm{E}\left[I_p I_p^* \sum_b \sum_{n=0}^{N_c-1} g_{a,b,n} g^*_{a,b,n}\right]}\right] \tag{29}$$

Because the amplitude tapering coefficients are real values then the PAPR of symbol a in the p–th transmitter equals:

$$\mathrm{PAPR}_{p,a}(\mathrm{dB}) = 10\log\left[\frac{\max\left[\sum_b \sum_{n=0}^{N_{c_b}-1} |g_{a,b,n}|^2\right]}{\mathrm{E}\left[\sum_b \sum_{n=0}^{N_{c_b}-1} |g_{a,b,n}|^2\right]}\right] \tag{30}$$

TABLE 3. PAPR of multiple beam CC-OFDM MIMO Radar for transmit element $p = 0$.

Codes	PAPR of the a-th symbol (dB)											
	1	2	3	4	5	6	7	8	9	10	11	12
Golay	6.0	6.3	5.8	5.8	6.8	5.9	7.4	6.9	6.3	6.7	6.9	6.6

The time domain signal transmitted from transmitter $p = 0$ contributing to 63 beams which are transmitted simultaneously using 8 sub bands is shown in Fig. 6. In Figure 6(b) with detailed observation from $t = 0$ to 0.1 ms (the signal period of symbol 1), the power computation of the transmitted symbol 1 give the maximum value of 15.4×10^{-4} and the average value of 3.84×10^{-4}. This gives the PAPR value around 4 which is equivalent to 6 dB. The PAPR results of the complete 12 CC OFDM symbols are shown in Table 3.

VI. AMBIGUITY FUNCTIONS

The ambiguity function of a conventional pulse radar is commonly defined as two-dimensional function of the propagation delay, τ, and the Doppler frequency, f_D:

$$\chi(\tau, f_D) = \int_{-\infty}^{\infty} x(t)x^*(t-\tau)e^{j2\pi f_D t}dt \tag{31}$$

However, the ambiguity function of CC-OFDM radar is a multi-dimensional function. Additionally, besides the two-dimensional function previously mentioned, the ambiguity function is also as a function of $\theta, \theta_0, \Delta t_b$, which are, respectively, the angular function, the target direction, and the time delay difference between the signals transmitted from successive elements for making beam b. Recalling the transmit signal from (14), and substituting into (31), the multidimensional ambiguity function of CC-OFDM MIMO radar can be written as:

$$\begin{aligned}\chi_{a,a'}(\tau, f_D, \theta, \theta_0, \Delta t_b) &= \chi_{a,a'}(\tau, f_D, \theta, \theta_0, \Delta t_b) \\ &= \sum_{n=0}^{N_{cb}-1} \sum_{p=-\frac{(N_t-1)}{2}}^{\frac{(N_t-1)}{2}} \sum_{m=0}^{N_{cb}-1} \sum_{q=-\frac{(N_r-1)}{2}}^{\frac{(N_r-1)}{2}} I_p I_q \\ &\times g_{a,b,n} g^*_{a',b',m} C'_{n,p,a,b} C'^*_{m,q,a'b'} \\ &\times e^{jp[\alpha(\theta_0)+\beta_{c,b})]} e^{-jq[\alpha(\theta)+\beta_{c,b'}]} \\ &\times e^{-j2\pi k(f_{a,n,b}-f_{a',m,b'})T_0} e^{j2\pi f_{a',m,b'}\tau} \\ &\times e^{j\pi(f_{a,n,b}-f_{a',m,b'}+f_D)T_0(2a'-1)} \\ &\times T_0 \,\mathrm{sinc}\,(\pi(f_{a,n,b} - f_{a',m,b'} + f_D)T_0)\end{aligned} \tag{32}$$

where p, q again denote the indexes of the transmit and receive elements respectively, I_p, I_q denote the amplitude tapering coefficients using Taylor distribution given to the p-th and q-th of the transmit and receive element, respectively, N_t, N_r are the number of transmit and receive elements respectively, $C'_{n,p,a,b}$ denotes the corrected phase of the transmitted CC-OFDM symbols, given to the n-th carrier frequency $f_{a,n,b}$ of the b-th beam, and $C'^*_{m,q,a',b'}$ denotes the complex conjugate of the correction phase of the received CC-OFDM symbols, given to the m-th carrier frequency of b'-th beam, which use subcarrier $f_{a',m,b'}$. For the surveillance radar example, we have $I_p = I_q$ and $N_t = N_r = 101$ and the ambiguity function is analyzed for $a' = a$,and $b' = b$ and due to orthogonality, it is analyzed when $n = m$ and $p = q$.

In the following, various ambiguity functions, each a function of beam, of delay and of Doppler frequency, are presented with transmitter time, sub band and codes scheduling for symbol-1 as visually described in Table 2. Based on the ambiguity function formulation in (32), the analyses are described as follows:

i. $\chi_{a'=a=1,b'=b}(\tau = 0, f_D = 0, \theta_0, \theta, \Delta t_b)$ is the radar ambiguity function analyzed by taking a variable value of θ_0 as a function of angular variable, θ. Fig. 7(a) shows the ambiguity function of CC-OFDM MIMO radar with the assumption that the target echo comes from the angular direction of θ_0 which coincide with the maximum of the beampattern in beam b. It can be seen that the beams are orthogonal. If it is seen in the 3D plot version in Fig.7(b), it can be seen that the magnitude of the ambiguity function at the edge beam where $\theta_0 = -43.1°$ is around half than the broadside beam. This is caused by the scan loss and because of the use of elements of $\cos(\theta)$-type pattern in the array.

ii. $\chi_{\theta_0,a'=a=1,b'=b}(\tau, f_D = 0, \theta, \Delta t_b)$ is the radar ambiguity function as a function of time delay variable, τ, and angular variable, θ. It is assumed that there is a non-moving target at a specific direction of θ_0. Observation is made for two different cases, the first one is when the target is at broadside ($\theta_0 = 0°$) and the second case is when the target is at the maximum scan angle ($\theta_0 = 43.1°$).
Fig. 8 and Fig. 9 show that the magnitudes of the ambiguity function are maximum at $\theta = 0°$ and $\theta = 43.1°$ respectively. Furthermore, when detail observation is done at $\theta = \theta_0$ axis, Fig. 8(c) and Fig. 9(c) show that with a bandwidth of 2.56 MHz, range resolution of 52 meter can be obtained either for a target at broadside or at the maximum scan angle. While in Fig. 8(b) and Fig. 9(b), respectively indicate that the angular resolution of 1.3° and 1.7° at the broadside and at the edge beam can be achieved. These results show that by using the proposed transmitter design, the surveillance radar requirement which has been mentioned in Table 1 can be fulfilled.

iii. $\chi_{a'=a=1,b'=b}(\tau, f_D, \theta = \theta_0, \Delta t_b)$ this ambiguity function as a function of time-delay variable τ, analyzed for a moving target which cause a Doppler frequency shift of f_D at the received beam b'. It is assumed that the target is located at a specified angular $\theta = \theta_0$. Fig 10(a) shows the target angular location at broadside, $\theta_0 = 0°$ and while Fig. 10(b) shows the target at the maximum scan angle $\theta_0 = 43.1°$, when a moving target is causing a Doppler frequency $-1\text{kHz} < f_D < 1$ kHz. It can be seen in Fig.10(c) that the magnitude of the ambiguity function is slightly decreasing due to the Doppler frequency. Even though the Doppler effect looks minor in here, it is important to specify a limit of the maximum Doppler frequency which will limit the maximum velocity that

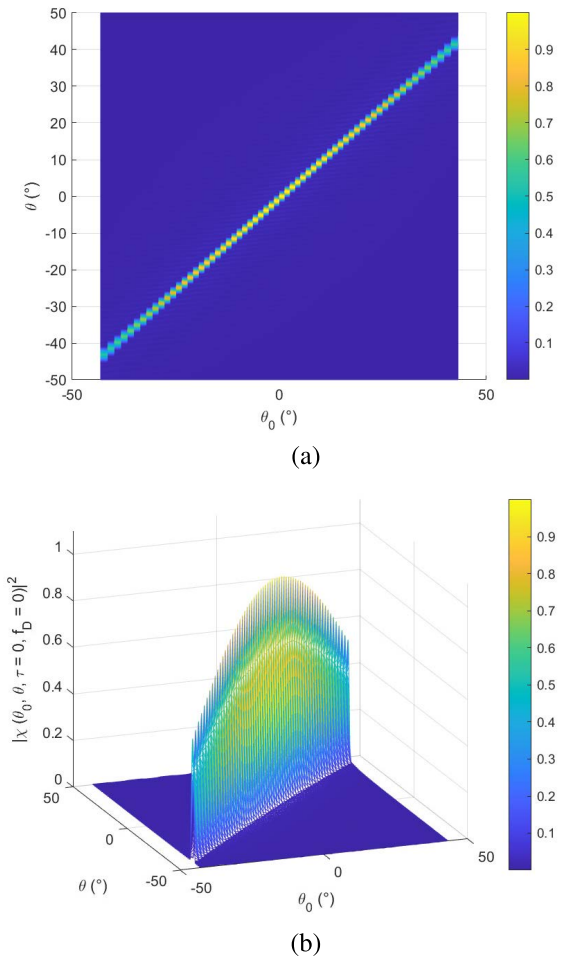

FIGURE 7. Ambiguity function of CC-OFDM MIMO radar as a function of θ and θ_0, when $\tau = 0$ and $f_D = 0$ in (a) 3D view from the top and (b) 3D view from the side.

the radar can detect. It should be limited to 10% of the spacing between the OFDM subcarrier, $f_{D,max} < 0.1\Delta f$.

VII. THE COUPLING BETWEEN CC-OFDM MULTI-BEAMS

A. THE COUPLING BETWEEN NEIGHBORING BEAMS

This section analyzes the coupling between beams which are transmitted simultaneously over the same period of symbol duration. Analysis is done to the beams transmitted on the first symbol period, with the scheduling as described in Table 2. It is necessary to make sure that the coupling between the multi-beam CC-OFDM which are transmitted simultaneously using limited bandwidth are low to avoid the probability of false alarm on radar receiver. In this paper, coupling analysis are done for near broadside and near edge beams (i.e., beams that spatially close to each other) and for co-channel beams (i.e., beams which are using the same subband frequency).

Fig. 11(a) shows that the coupling between the broadside beam with the nearest beams (i.e. $b = -1, 1$) is -30 dB. Similar to the edge beam case on Fig. 11(b), the coupling between the edge beam, $b = -31$ and beam $b = -30$ is also -30 dB. This result is caused by the Taylor amplitude

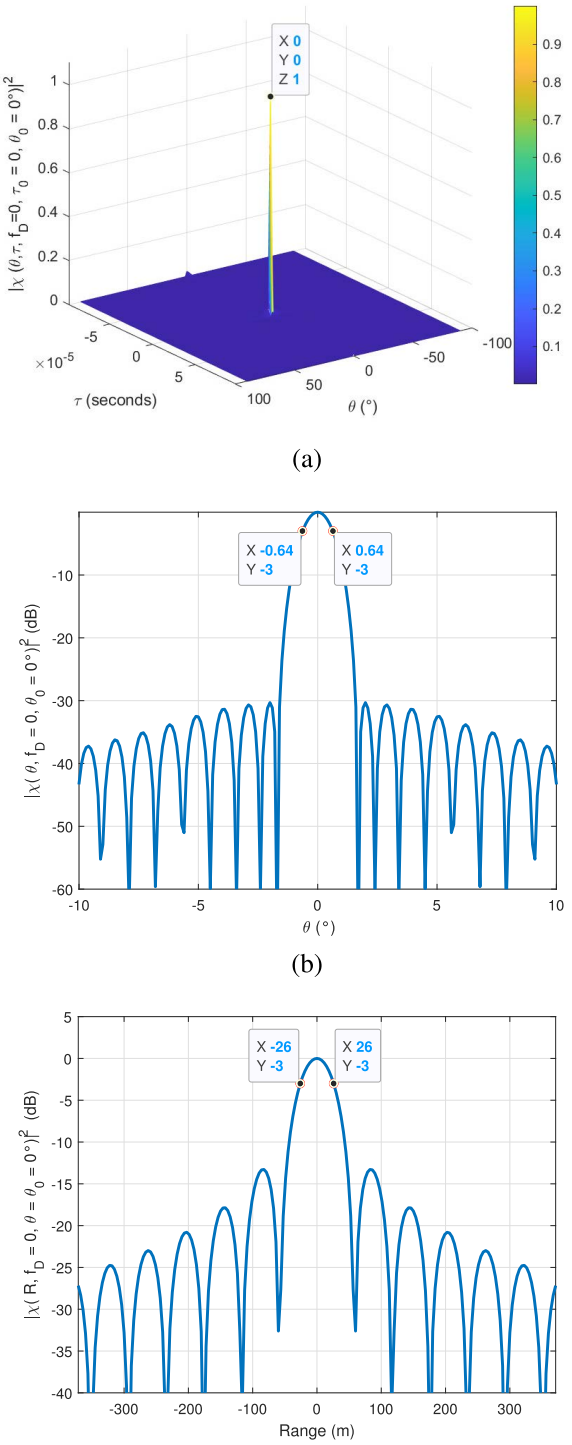

FIGURE 8. Ambiguity function diagram for a target at broadside, $\theta_0 = 0°$, (a) as a function of time delay τ and angular θ, (b) angular resolution at broadside, axis, and (c) radar range resolution seen from $\theta = \theta_0$.

tapering given to the array elements for SLL suppression to -30 dB. A lower coupling can be obtained by giving a different amplitude tapering coefficient, however it must be taken into consideration that minimizing the SLL gives consequence than the gain is decreased, and the beamwidth gets wider.

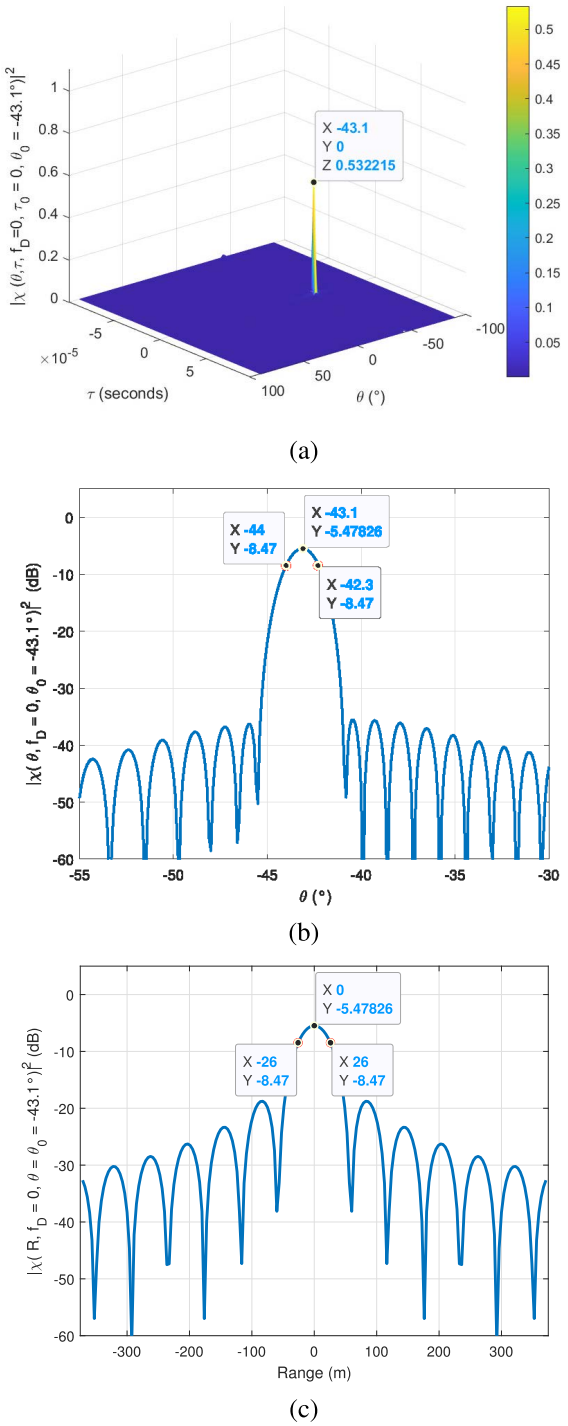

FIGURE 9. Ambiguity function diagram for a target at maximum scan angle $\theta_0 = 43.1°$, (a) as a function of time delay τ and angular θ, (b) Radar angular resolution, and, (c) radar range resolution at maximum scan angle $\theta_0 = 43.1°$.

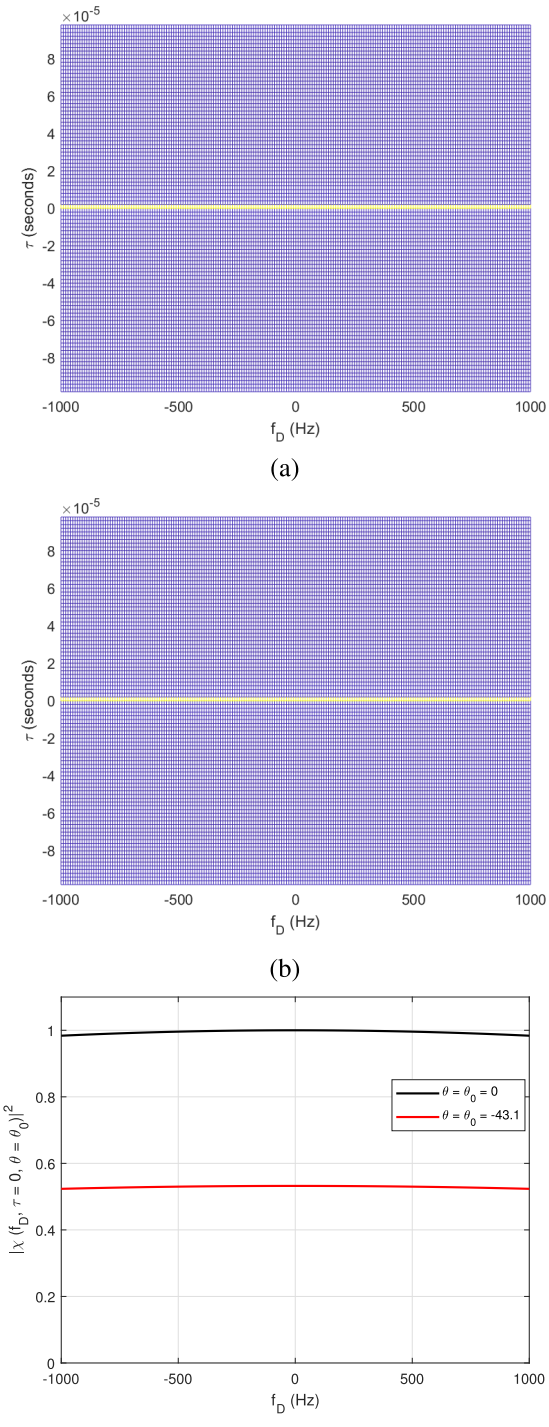

FIGURE 10. Ambiguity function as a function of Doppler frequency and time delay variable τ when the target is at: (a) broadside, (b) the edge, and (c) the detailed observation on the doppler effect at $\theta = \theta_0$ and $\tau = 0$.

Based on the subband frequency scheduling in Table 2, these neighboring beams are transmitted using a different sub-band frequency. Hence the beams which are spatially close to each other could get additional orthogonality to have a low-coupling characteristics between neighboring beams. Another additional orthogonality comes from the use of unique Golay codes for the beams which are transmitted simultaneously at the same symbol duration. All of these arrangements are made to provide a high isolation between neighboring beams.

B. THE COUPLING BETWEEN CO-CHANNEL BEAMS

Ambiguity function of the co-channel beams in sub band 1 and sub band 8 are consecutively shown on the in

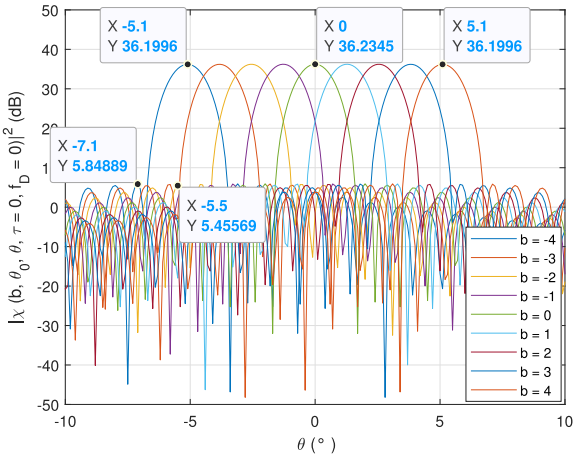

(a)

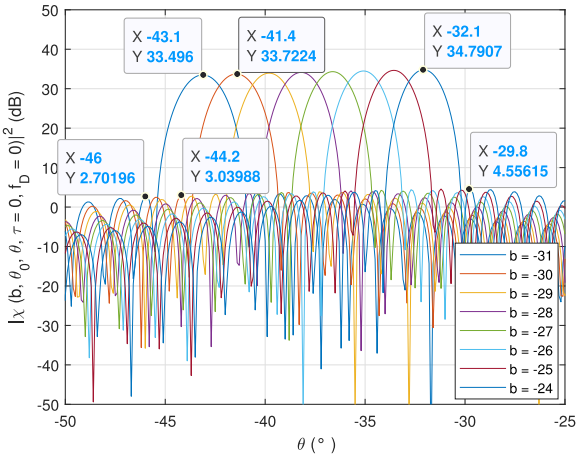

(b)

FIGURE 11. The ambiguity function of CC-OFDM MIMO radar, when $\tau = 0$ and $f_D = 0$ at: (a) neighboring beams of the broadside beam, and (b) the edge beam.

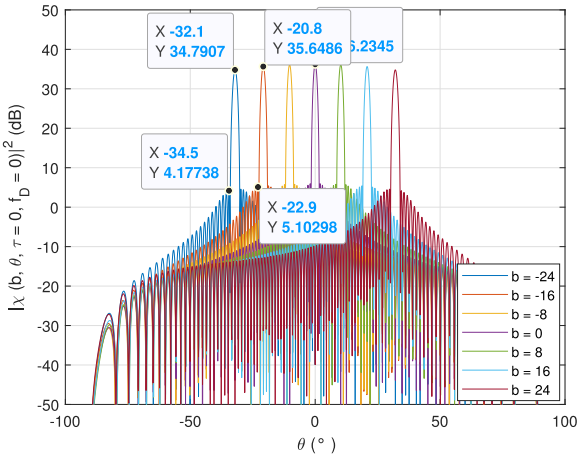

(a)

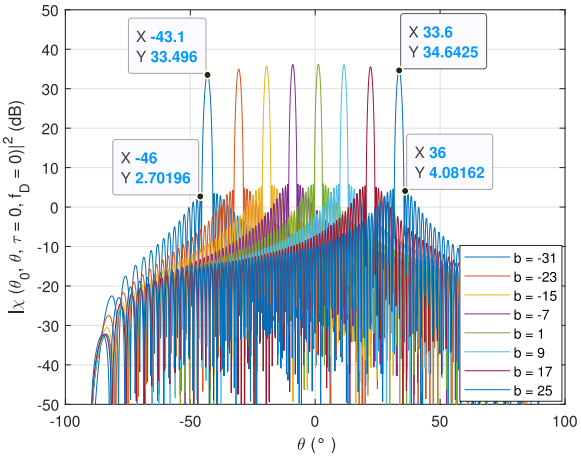

(b)

FIGURE 12. The ambiguity function of CC-OFDM MIMO radar for: (a) co-channel beams of the broadside beam, and (b) the edge beam when $\tau = 0$ and $f_D = 0$.

Fig. 12(a) and Fig. 12(b). It can be seen that the SLL of the co-channel beams in near broadside or near edge are around −30 dB. These co-channel beams lack orthogonality because of the subband frequency reuse. However, these co-channel beams are also provided with unique Golay codes for orthogonality. Besides that, the nearest co-channel beams are spatially separated at least 10°, which result in a low-coupling characteristics between the transmitted co-channel beams.

C. THE COUPLING BETWEEN BEAMS WHICH ARE USING THE SAME GOLAY CODES

Fig. 13 shows the ambiguity function of symbol 1, 5 and 9 of beam 5, 8 and 2 respectively. Recalling the transmit scheduling in Table 2, these three beams will be transmitted using the same Golay codes. Even though the beams are using the same code, the beam isolation is still as low as −30 dB because the three beams are transmitted using a different subband frequency. Therefore, all the coupling between beams or symbol which are using the same codes are very low.

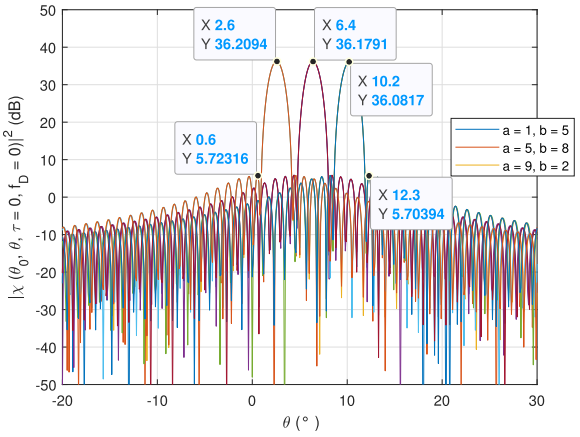

FIGURE 13. The ambiguity function of CC-OFDM MIMO radar for beams which are using the same Golay code.

D. THE COUPLING BETWEEN 63 BEAMS

The ambiguity function of the 63 beams of CC-OFDM MIMO radar using 101 ULA with Taylor amplitude tapering for sidelobe level suppression to −30 dB is shown in Fig. 14. The ambiguity function analysis is done over the transmission

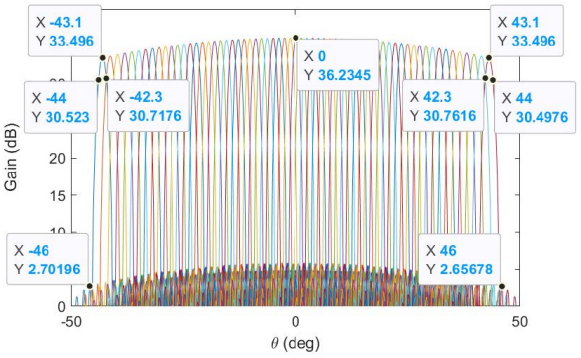

FIGURE 14. Multi beampattern of CC-OFDM MIMO radar using 101 ULA with Taylor amplitude tapering for SLL suppression of −30 dB when $\tau = 0$ and $f_D = 0$.

period of the first symbol (0-0.1 ms), when $\tau = 0$ and $f_D = 0$. It can be seen that the coupling between the 63 transmitted beams of symbol 1, starting from beam $b = -31$ up to $b = 31$ is around −30 dB.

VIII. DISCUSSIONS

An example of the transmitter design for a long-range surveillance radar has been described to clarify the concept and demonstrate the potential issues and advantages of the CC-OFDM MIMO radar. The radar is designed using 20.48 MHz bandwidth, which are divided into 8 sub bands with a bandwidth of 2.56 MHz each. Therefore, the expected range resolution of each beam is around 60 meters. From the ambiguity function result, the range resolution requirement of less than 60 meter could be obtained both for broadside and maximum scan angle beams. Range resolution always mainly depends on the bandwidth, hence, there will always be a trade-off between the range resolution requirements and the available bandwidth.

Based on the system requirement that 63 beams are needed for radar coverage from −45° to 45°, these 8 sub bands must be reused by 8 beams in average. As a consequence of reusing each sub band for 8 beams, the beam isolation might worsen for the co-channel beams, which can result in false alarm in the nearest co-channel beam. High beam isolation can be obtained by using different sub band for each beam, however because the bandwidth is limited, sub band reuse becomes inevitable. For the multi-beam case, by arranging the sub band and codes allocation of the beams, the ambiguity function analysis shows that the beam isolation between the transmitted neighboring beam and the transmitted co-channel beams is around −30 dB. The symbols serial arrangement in each beam allows the radar to detect targets up to 180 km in that beam direction.

From the description and discussion about the concept of CC-OFDM and its T-R module in Sections II-III, it can be seen that combining CC and OFDM waveform makes it possible to adopt a software defined radar (SDR). The idea of SDR is to have a radar that most part of the signal processing can be done by software, hence it can be a multi-purpose radar. It is hence possible to use the same hardware components for different radar applications. From Fig. 4, the WG and the digital signal processor at each transmitter are designed and controlled by software. Based on the mission requirement, the CC-OFDM waveform can be modified in a more convenient way. Adjustments on the design can be done according to the purpose of the radar by changing some of the design parameters in software and keep the same hardware components. Of course, not everything can be replaced with software, some radar parameters will still depend on the hardware. For instance, the carrier frequency will depend on the RF analog chain, while the radar beamwidth will mainly depend on the arrays. But the characteristic of the output beampattern, such as its sidelobe level, and the design of the multiple simultaneously beam, including the beam isolation, the range resolution, the Doppler resolution, those parameters can be modified and optimized based on the characteristic of the target of interest. Some of the radar specifications that can be achieved by modifying some of the CC-OFDM waveform parameters are as follows:

- **The maximum unambiguous range** for conventional OFDM radar is mainly limited by the spacing between the OFDM subcarriers. However, one could extend the maximum unambiguous range of the radar by sending multiple successive orthogonal CC-OFDM symbols containing orthogonal Golay codes. How many symbols that must be sent will depend on how far the maximum unambiguous range is that the application requires.
- **The maximum velocity** depends on the frequency spacing between the OFDM sub carriers, because there is a limitation on the maximum Doppler frequency, that it should not be more than 10% of the sub carrier spacing.
- **The angular coverage requirement** will define the array requirements and the multiple beams design. With regards to the beamwidth, there is not much that can be done, since it depends on the array. However, the angular coverage is related to the number of beams that must be generated simultaneously, which can be defined from the CC-OFDM waveforms. Allocation and arrangements of the available bandwidth for creating those beams must be considered on the design, which can be done in convenient way in the frequency domain stage of the OFDM waveform.
- **Range resolution** of the radar in every beam direction will depend on the bandwidth allocated for those beams. With OFDM, it can be done easily by software by dividing the total available bandwidth into several sub-bands with each sub band have a minimum bandwidth for the required range resolution.
- **Doppler resolution** can be fulfilled by sending a train of orthogonal symbols, i.e. a frame, repeatedly to allow evaluation of the phase change between the same symbols in successive frames.
- **Beam isolation** is a very crucial requirement that needs special attention in CC-OFDM, especially when the available bandwidth is limited, so that there are beams which are transmitted simultaneously using the

same frequency. This will cause couplings between the co-channel beams. Hence, in the scheduling of the sub band frequency reuse, the beam spacing between co-channel beams must be long enough to minimize the coupling effects.

IX. CONCLUSION

A transmitter design for CC-OFDM MIMO radar has been introduced. The radar concept has been shown to offer various advantages, including the multiple beams covering a wide view, the long-range target detection capability and the use of low-power amplifiers. All of these advantages are the result of the combination of several technologies, primarily the use of the MIMO concept with OFDM waveforms generated in different subbands and coded by CC across the array azimuth, coupled with the use of Golay codes to reduce PAPR and to improve orthogonality between symbols. Orthogonalities among symbols and beams result from the combined effects of Golay codes, subbands and amplitude tapering of the elements across the azimuth, which in turn allow long-range target detection and better angular accuracy. The azimuth angular resolution depends on the number of azimuthal elements and improved by the arrangement of adjacent beams based on intersection of the 3-dB directivity curves. The resolution and maximum unambiguity in range depends on the subband width and subcarrier spacing, whereas those in Doppler depends on the number of frames used in the processing and the interval between frames. SNR for target range detection can be optimized by varying the number of orthogonal symbols per frame.

Since most processes mainly depend on the arrangement of the transmitted waveforms and the processing of the received echoes, adoption of the SDR that provides general-purpose digital signal processing algorithms that can be controlled by software becomes feasible and attractive. The hardware platform consisting of multiple transmit-receive boards including antenna elements that comprise the azimuth linear array and the corresponding RF apparatuses. The adoption of digital waveforms generators and digital signal processors, which are essentially materialized in SDR, makes it possible for the radar to change its configuration and parameters for different mission requirements. Finally, an example of the transmitter design for long-range surveillance radar has been described to clarify the concept and demonstrate the potential advantages of the CC-OFDM MIMO radar. By using the proposed design, a range resolution of 52 meter and an azimuth resolution of 1.7° can be achieved. For the multi-beam scheme, the beam isolation of −30 dB can be achieved for both between the co-channel beams and between the neighboring beams.

The receiver design of CC-OFDM radar, including the beam, range and Doppler processing of the received signal will be discussed in a separate paper.

REFERENCES

[1] M. I. Skolnik, *Radar Handbook*, 3rd ed. New York, NY, USA: McGraw-Hill, 2008.

[2] C. A. Balanis, *Antenna Theory: Analysis and Design*, 3rd ed. Hoboken, NJ, USA: Wiley, 2012.

[3] D. Gromek, P. Samczyński, J. Misiurewicz, M. Malanowski, K. Kulpa, A. Gromek, A. Gadós, A. Jarzębska, and M. Smolarczyk, "Implementation and results of new high resolution SAR modes for an airborne maritime patrol radar," *Int. J. Electron. Telecommun.*, vol. 59, no. 3, pp. 213–218, Sep. 2013, doi: 10.2478/eletel-2013-0025.

[4] M. Losacco, M. Schiaffino, F. Perini, L. Lama, A. Mazro, D. Cutaiar, J. Borg, W. Villadei, M. Reali, P. Di Lizia, M. Massari, G. Bianchi, G. Pupillo, A. Mattana, G. Naldi, C. Bertolotti, and M. Roma, "The multibeam radar sensor BIRALES: Performance assessment for space surveillance and tracking," in *Proc. IEEE Aerosp. Conf.*, Mar. 2019, pp. 1–14.

[5] J. Moghaddasi and K. Wu, "Multifunctional transceiver for future radar sensing and radio communicating data-fusion platform," *IEEE Access*, vol. 4, pp. 818–838, 2016, doi: 10.1109/ACCESS.2016.2530979.

[6] H. Krishnaswamy and H. Hashemi, "A 4-channel 4-beam 24-to-26 GHz spatio-temporal RAKE radar transceiver in 90 nm CMOS for vehicular radar applications," in *IEEE Int. Solid-State Circuits Conf. (ISSCC) Dig. Tech. Papers*, Feb. 2010, pp. 214–215, doi: 10.1109/ISSCC.2010.5433954.

[7] T. X. H. Luo, W. W. L. Lai, R. K. W. Chang, and D. Goodman, "GPR imaging criteria," *J. Appl. Geophysics*, vol. 165, pp. 37–48, Jun. 2019, doi: 10.1016/j.jappgeo.2019.04.008.

[8] K. B. Cooper, R. J. Dengler, N. Llombart, B. Thomas, G. Chattopadhyay, and P. H. Siegel, "THz imaging radar for standoff personnel screening," *IEEE Trans. THz Sci. Technol.*, vol. 1, no. 1, pp. 169–182, Sep. 2011, doi: 10.1109/TTHZ.2011.2159556.

[9] S. D. Liyanaarachchi, C. Baquero Barneto, T. Riihonen, M. Heino, and M. Valkama, "Joint multi-user communication and MIMO radar through full-duplex hybrid beamforming," in *Proc. 1st IEEE Int. Online Symp. Joint Commun. Sens. (JC&S)*, Feb. 2021, pp. 1–5, doi: 10.1109/JCS52304.2021.9376319.

[10] X. Liu, T. Huang, N. Shlezinger, Y. Liu, J. Zhou, and Y. C. Eldar, "Joint transmit beamforming for multiuser MIMO communications and MIMO radar," *IEEE Trans. Signal Process.*, vol. 68, pp. 3929–3944, 2020, doi: 10.1109/TSP.2020.3004739.

[11] G. Krieger, "MIMO-SAR: Opportunities and pitfalls," *IEEE Trans. Geosci. Remote Sens.*, vol. 52, no. 5, pp. 2628–2645, May 2014, doi: 10.1109/TGRS.2013.2263934.

[12] D.-S. Jang and H.-L. Choi, "Interleaved radar pulse scheduling for multi-target tracking with multiple simultaneous receive beams," *IEEE Trans. Aerosp. Electron. Syst.*, vol. 55, no. 3, pp. 1301–1318, Jun. 2019, doi: 10.1109/TAES.2018.2869505.

[13] K. Ying, Z. Gao, S. Lyu, Y. Wu, H. Wang, and M.-S. Alouini, "GMD-based hybrid beamforming for large reconfigurable intelligent surface assisted millimeter-wave massive MIMO," *IEEE Access*, vol. 8, pp. 19530–19539, 2020, doi: 10.1109/ACCESS.2020.2968456.

[14] K. R. Xiang, F. C. Chen, Q. X. Chu, and M. J. Lancaster, "A broadband 3×4 Butler matrix and its application in multi-beam antenna arrays," *IEEE Trans. Antennas Propag.*, vol. 67, no. 12, pp. 7622–7627, Aug. 2019, doi: 10.1109/TAP.2019.2934793.

[15] J. P. Shelton, "Fast Fourier transforms and Butler matrices," *Proc. IEEE*, vol. 56, no. 3, p. 350, Mar. 1968, doi: 10.1109/PROC.1968.6302.

[16] H. Moody, "The systematic design of the Butler matrix," *IEEE Trans. Antennas Propag.*, vol. AP-12, no. 6, pp. 786–788, Nov. 1964, doi: 10.1109/TAP.1964.1138319.

[17] X. Wei, T. Cheng, and H. Peng, "Adaptive resource management in multi-target tracking for collocated MIMO radar with simultaneous multibeam," in *Proc. 22th Int. Conf. Inf. Fusion (FUSION)*, Jul. 2019, pp. 1–8.

[18] E. Fishler, A. Haimovich, R. S. Blum, L. J. Cimini, D. Chizhik, and R. A. Valenzuela, "Spatial diversity in radars—Models and detection performance," *IEEE Trans. Signal Process.*, vol. 54, no. 3, pp. 823–838, Mar. 2006, doi: 10.1109/TSP.2005.862813.

[19] W. L. Melvin and J. A. Scheer, *Principles of Modern Radar: Advanced Techniques*, vol. 2. Rijeka, Croatia: SciTech, 2013.

[20] J. Li and P. Stoica, "MIMO radar with colocated antennas," *IEEE Signal Process. Mag.*, vol. 24, no. 5, pp. 106–114, Sep. 2007, doi: 10.1109/MSP.2007.904812.

[21] J.-D. Zhu, J.-L. Li, X.-D. Gao, L.-B. Ye, and H.-Y. Dai, "Adaptive threshold detection and estimation of linear frequency-modulated continuous-wave signals based on periodic fractional Fourier transform," *Circuits, Syst., Signal Process.*, vol. 35, no. 7, pp. 2502–2517, Jul. 2016, doi: 10.1007/s00034-015-0152-z.

[22] A. S. Paulus, W. L. Melvin, and D. B. Williams, "Multichannel GMTI techniques to enhance integration of temporal signal energy for improved target detection," *IET Radar, Sonar Navigat.*, vol. 11, no. 3, pp. 395–403, Mar. 2017, doi: 10.1049/iet-rsn.2016.0082.
[23] L. Kocjancic, A. Balleri, and T. Merlet, "Multibeam radar based on linear frequency modulated waveform diversity," *IET Radar, Sonar Navigat.*, vol. 12, no. 11, pp. 1320–1329, Nov. 2018, doi: 10.1049/iet-rsn.2018.5029.
[24] W.-Q. Wang, "Frequency diverse array antenna: New opportunities," *IEEE Antennas Propag. Mag.*, vol. 57, no. 2, pp. 145–152, Apr. 2015, doi: 10.1109/MAP.2015.2414692.
[25] Y. Xu and K.-M. Luk, "Enhanced transmit–receive beamforming for frequency diverse array," *IEEE Trans. Antennas Propag.*, vol. 68, no. 7, pp. 5344–5352, Jul. 2020, doi: 10.1109/TAP.2020.2977717.
[26] B. Donnet and I. Longstaff, "Combining MIMO radar with OFDM communications," in *Proc. Eur. Radar Conf.*, Sep. 2006, doi: 10.1109/EURAD.2006.280267.
[27] C. Sturm, E. Pancera, T. Zwick, and W. Wiesbeck, "A novel approach to OFDM radar processing," in *Proc. IEEE Radar Conf.*, 2009, doi: 10.1109/RADAR.2009.4977002.
[28] Y. L. Sit, T. T. Nguyen, and T. Zwick, "3D radar imaging with a MIMO OFDM-based radar," in *Proc. Asia–Pacific Microw. Conf. Proc. (APMC)*, Nov. 2013, pp. 68–70, doi: 10.1109/APMC.2013.6695193.
[29] G. Hakobyan, M. Girma, X. Li, N. Tammireddy, and B. Yang, "Repeated symbols OFDM-MIMO radar at 24 GHz," in *Proc. Eur. Radar Conf. (EuRAD)*, 2016, pp. 249–252.
[30] G. Hakobyan, M. Ulrich, and B. Yang, "OFDM-MIMO radar with optimized nonequidistant subcarrier interleaving," *IEEE Trans. Aerosp. Electron. Syst.*, vol. 56, no. 1, pp. 572–584, Feb. 2020, doi: 10.1109/TAES.2019.2920044.
[31] C. Knill, F. Embacher, B. Schweizer, S. Stephany, and C. Waldschmidt, "Coded OFDM waveforms for MIMO radars," *IEEE Trans. Veh. Technol.*, vol. 70, no. 9, pp. 8769–8780, Sep. 2021, doi: 10.1109/TVT.2021.3073268.
[32] K. Roussel, G. Babur, and F. Le Chevalier, "Optimization of low sidelobes radar waveforms: Circulating codes," in *Proc. Int. Radar Conf.*, Oct. 2014, pp. 1–6, doi: 10.1109/RADAR.2014.7060290.
[33] L. Nan, Z. Zhenghe, and Z. Linrang, "Waveform analytic design method for transmit beampattern synthesis of circulating coded MIMO radar," *IEEE Sensors J.*, vol. 20, no. 3, pp. 1485–1498, Feb. 2020, doi: 10.1109/JSEN.2019.2946643.
[34] K. V. Caekenberghe, K. Brakora, and K. Sarabandi, "OFDM frequency scanning radar," Google Patent US7 994 969 B2, Sep. 21, 2007.
[35] A. Hassanien and S. A. Vorobyov, "Phased-MIMO radar: A tradeoff between phased-array and MIMO radars," *IEEE Trans. Signal Process.*, vol. 58, no. 6, pp. 3137–3151, Jun. 2010, doi: 10.1109/TSP.2010.2043976.
[36] S. Tahcfulloh and G. Hendrantoro, "FPMIMO: A general MIMO structure with overlapping subarrays for various radar applications," *IEEE Access*, vol. 8, pp. 11248–11267, 2020, doi: 10.1109/ACCESS.2020.2965192.
[37] S. Yan, M. Xie, H. Sun, and Y. Shang, "Maximum secrecy-key capacity design for amplify- and-forward relays in secure cooperative networks," in *Proc. IEEE 88th Veh. Technol. Conf. (VTC-Fall)*, Aug. 2018, pp. 1–6, doi: 10.1109/VTCFall.2018.8690748.
[38] M. Alam, Z. O. Alhekail, S. Al-Humaidi, and K. Jamil, "A multi-band multi-beam software-defined passive radar. Part II: Signal processing," in *Proc. IET Int. Conf. Radar Syst. (Radar)*, Oct. 2012, pp. 1–5, doi: 10.1049/cp.2012.1582.
[39] G. Babur, P. Aubry, and F. Le Chevalier, "Space-time radar waveforms: Circulating codes," *J. Electr. Comput. Eng.*, vol. 2013, pp. 1–8, 2013, doi: 10.1155/2013/809691.
[40] C. Sturm and W. Wiesbeck, "Waveform design and signal processing aspects for fusion of wireless communications and radar sensing," *Proc. IEEE*, vol. 99, no. 7, pp. 1236–1259, Jul. 2011, doi: 10.1109/JPROC.2011.2131110.
[41] G. E. A. Franken, H. Nikookar, and P. Van Genderen, "Doppler tolerance of OFDM-coded radar signals," *Proc. Eur. Radar Conf.*, Sep. 2006, pp. 108–111, doi: 10.1109/EURAD.2006.280285.
[42] A. S. Paulus, W. L. Melvin, and D. B. Williams, "Multistage algorithm for single-channel extended-dwell signal integration," *IEEE Trans. Aerosp. Electron. Syst.*, vol. 53, no. 6, pp. 2998–3007, Dec. 2017, doi: 10.1109/TAES.2017.2724358.
[43] A. S. Paulus, W. L. Melvin, and D. B. Williams, "Improved target detection through extended dwell time algorithm," in *Proc. IEEE Radar Conf. (RadarCon)*, May 2015, pp. 0484–0489, doi: 10.1109/RADAR.2015.7131047.

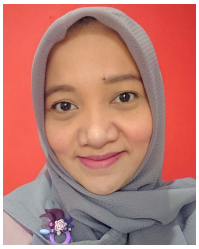

DEVY KUSWIDIASTUTI (Student Member, IEEE) was born in Indonesia, in September 1981. She received the B.Eng. degree in electrical engineering from the Institut Teknologi Sepuluh Nopember (ITS), Indonesia, in 2004, and the M.Sc. degree from Hochschule Darmstadt, Germany, in 2008. She is currently pursuing the Ph.D. degree with ITS. She was with the Research and Development Engineering Department, Panasonic Shikoku Electronics, Indonesia, from 2004 to 2006. She works as a Lecturer with ITS. Her current research interests include MIMO radar and array signal processing.

L. P. LIGTHART (Life Fellow, IEEE) was born in The Netherlands, in September 1946. He received the degree *(cum laude)* in engineering and the Ph.D. degree from the Delft University of Technology. Since 1988, he has been the Chair of MW transmission, remote sensing, radar, and positioning and navigation with the Delft University of Technology. He founded the IRCTR at Delft University, where he is currently an Emeritus Professor, a Guest Professor with universities in Indonesia and China, and the Chairperson of CONASENSE. He teaches various courses on radar and remote sensing in antennas and has published more than 650 articles, various book chapters, and books. He has supervised more than 50 Ph.D. students. His research interests include antennas and propagation, radar and remote sensing, satellite, and mobile and radio communications. He is a member BoG of the IEEE-AESS, a fellow of IET, and the Academician of the Russian Academy of Transport. He is also a Founding Member of the EuMA; has chaired 1st EuMW, in 1998; and is an Initiated EuRAD, in 2004. He received Honorary Doctorates at MSTUCA, Moscow; Tomsk State University; and MTA Romania.

GAMANTYO HENDRANTORO (Senior Member, IEEE) was born in Jombang Regency, Indonesia, in November 1970. He received the B.Eng. degree in electrical engineering from the Institut Teknologi Sepuluh Nopember (ITS), Surabaya, Indonesia, in 1992, and the M.Eng. and Ph.D. degrees in electrical engineering from Carleton University, Ottawa, ON, Canada, in 1997 and 2001, respectively. He is currently a Professor with the Department of Electrical Engineering, ITS. His current research interests include radio propagation channel modeling and wireless communications. He has been involved in various studies, including investigation into millimeter-wave propagation, channel modeling and wireless systems for tropical areas, studies on HF skywave channels and communications in equatorial regions, and the development of radar array and signal processing.